Tectonic and oceanographic process interactions archived in the Late Cretaceous to Recent deep-marine stratigraphy on the Exmouth Plateau, offshore NW Australia

Harya D. Nugraha[1], Christopher A-L. Jackson[1], Howard D. Johnson[1], David M. Hodgson[2], and Matthew T. Reeve[1]

[1]*Basins Research Group, Department of Earth Science and Engineering, Imperial College, London*

[2]*Stratigraphy Group, School of Earth and Environment, University of Leeds, Leeds*

**email: harya.nugraha14@imperial.ac.uk*

6818 words (excluding references: 3129; figure captions: 673)

ABSTRACT

Deep-marine deposits provide a valuable archive of process interactions between sediment gravity flows, pelagic sedimentation, and thermo-haline bottom-currents. Stratigraphic successions can also record plate-scale tectonic processes (e.g. continental breakup and shortening) that impact long-term ocean circulation patterns, including changes in climate and biodiversity. One such setting is the Exmouth Plateau, offshore NW Australia, which has been a relatively stable, fine-grained carbonate-dominated continental margin from the Late Cretaceous to the Recent. During this time, the Exmouth Plateau was located between areas of continental breakup and shortening. We combine extensive 2D (~40,000 km) and 3D (3,627 km^2) seismic reflection data with lithologic and biostratigraphic information from wells to reconstruct the tectonic and oceanographic evolution of this deep-marine margin. We identified three large-scale seismic units (SUs): (1) SU-1 (Late Cretaceous) is up to 500 m-thick, and characterised by NE-SW-trending, slope-normal elongate depocentres (c. 200 km long and 70 km wide), with erosional surfaces at their bases and tops, which are interpreted as the result of contour-parallel bottom-currents, coeval with the onset of opening of the Southern Ocean; (2) SU-2 (Palaeocene – Late Miocene) is up to 800 m-thick and characterised by (i) very large (amplitude, c. 40 m and wavelength, c. 3 km), SW-migrating, NW-SE-trending sediment waves, and (ii) large (4 km-wide, 100 m-deep), NE-SW-trending scours that flank the sediment waves, which may reflect an intensification of NE-flowing bottom currents during a relative sea-level fall following the establishment of circumpolar-ocean current around Antarctica; and (3) SU-3 (Late Miocene – Recent) is up to 1000 m-thick and is dominated by large (up to 100 km^3) mass-transport complexes (MTCs), which were derived from the continental margin (to the east) and the Exmouth Plateau Arch (to the west), and accumulated mainly in the adjacent Kangaroo Syncline. SU-3 deposition is dominated by gravity flow and hemipelagic processes, and lacks evidence for bottom-current activity; this change in depositional style may be linked to tectonically-induced seabed tilting and folding caused by collision and subduction along the northern margin of the Australian plate. Hence, the stratigraphic record of this relatively low-energy, fine-grained dominated passive continental margin provides a rich archive of plate-scale regional geological events occurring along the distant southern (2000 km away) and northern (1500 km away) margins of the Australian plate.

Keywords: Tectonics and sedimentation, palaeo-oceanography, deep marine, seismic reflection, bottom current, contourites, MTCs.

1. Introduction

Sedimentary successions in deep-marine basins provide valuable archives of process interactions between gravity-driven processes (i.e. down-slope processes), (hemi)pelagic sedimentation, and thermohaline bottom-current circulations (i.e. along-slope processes) (e.g. Pickering *et al.*, 1989; Huneke & Mulder, 2010; Llave *et al.*, 2018). One of these processes may dominate, both spatially and temporally (Faugères & Stow, 1993; Hernández-Molina *et al.*, 2006b; Campbell & Deptuck, 2012). For instance, periods of intense tectonism may be recorded by repeated deposition of mass-transport complexes (MTCs) spatially associated with specific structures (Hampton *et al.*, 1996; Masson *et al.*, 2010; Ortiz-Karpf *et al.*, 2016; Pérez *et al.*, 2016). In contrast, during periods dominated by the activity of intense, along-slope currents may produce contourite depositional systems, from which oceanographic and/or palaeo-oceanographic processes can be inferred (Pickering *et al.*, 1989; Viana *et al.*, 1998; Hernández-Molina *et al.*, 2006b; Uenzelmann-Neben, 2006;

Ercilla *et al.*, 2016; Hernández-Molina *et al.*, 2016; Pérez *et al.*, 2017). Therefore, deep-marine stratigraphy can record tectonic and oceanographic processes, including periods of continental rifting and collision that may result in the opening and closing, respectively, of ocean gateways (Faugères & Stow, 2008; Knutz, 2008; Hernández-Molina *et al.*, 2016; Pérez *et al.*, 2017).

To date, bottom-current deposits (i.e. contourites) have been used as proxies to reconstruct: (i) the history of palaeo-oceanographic and/or palaeoclimatic changes (e.g. Mulder *et al.*, 2002; Uenzelmann-Neben, 2002; Hernández-Molina *et al.*, 2006a; Uenzelmann-Neben & Gohl, 2012; Vandorpe *et al.*, 2014; Gruetzner & Uenzelmann-Neben, 2016; Pérez *et al.*, 2017); and (ii) the contribution of oceanographic processes on continental margins and deep-marine basins evolution (e.g. Johnson & Damuth, 1979; Reed *et al.*, 1987; Hernández-Molina *et al.*, 2006b; García *et al.*, 2009; Martos *et al.*, 2013; Pérez *et al.*, 2014; Soares *et al.*, 2014; Gong *et al.*, 2017; Pérez *et al.*, 2017). On the other hand, contribution of gravity-driven deposits (e.g. MTCs) to continental margins development have also been used to reconstruct tectono-sedimentary evolution in: (i) passive margins (e.g. Heinio & Davies, 2006; Gamboa *et al.*, 2010; Clark *et al.*, 2012; Armandita *et al.*, 2015; Scarselli *et al.*, 2016; Thöle *et al.*, 2016); and (ii) active margins (e.g. Romero-Otero *et al.*, 2010; Vinnels *et al.*, 2010; Richardson *et al.*, 2011; Völker *et al.*, 2012; Alfaro & Holz, 2014; Pérez *et al.*, 2016). In addition, process interactions between these along- and downslope processes have also been documented (e.g. Kähler & Stow, 1998; Michels *et al.*, 2001; Akhurst *et al.*, 2002; Mulder *et al.*, 2006; Salles *et al.*, 2010). For example, not only bottom-currents can rework gravity-driven deposits (e.g. Shanmugam *et al.*, 1993; Marchès *et al.*, 2010), but they also can destabilise a slope and eventually trigger gravity-driven processes (e.g. Esmerode *et al.*, 2008; Martorelli *et al.*, 2016). However, how deep-marine stratigraphy of relatively stable passive margins (i.e. without salt or mud tectonics) records the evolution of tectonic and oceanographic process interactions along distant (>1000 km) plate-tectonic margins is poorly-documented.

The Exmouth Plateau provides an opportunity to examine how deep-marine stratigraphy archives plate-scale tectonic and oceanographic events, since it is located between areas of rifting and collision along the southern and northern margins of the Australian plate, respectively. The Exmouth Plateau is a continental block on the north-western Australian continental margin (Fig. 1), which has been a carbonate-dominated deep-marine basin from the Late Cretaceous to Recent (Fig. 2) (Exon *et al.*, 1992; Haq *et al.*, 1992). Although the regional tectonic development of the Exmouth Plateau and surrounding areas is well-documented (e.g. Karner & Driscoll, 1999; Cathro & Karner, 2006; Keep *et al.*, 2007; Müller *et al.*, 2012), the sedimentary processes operating during the late post-rift megasequence (Late Cretaceous to Present-day) remain poorly-understood. We here use a high-quality, extensive (cumulative length of ~40.000 km) time-migrated 2D seismic reflection dataset to: (i) define regional basin structure; (ii) characterise depocentre style and migration resulting from, and recording, a range of tectonic events; and (iii) infer depositional style via seismic facies analysis. In addition, a time-migrated 3D seismic reflection volume (3627 km^2) is used to understand erosional and depositional processes in a more hydrodynamically complex area. We also use well data to constrain lithology, age, and palaeo-water depth.

We demonstrate that the offshore seismic stratigraphy provides a proven record of tectonic and oceanographic process interactions. The deep-marine stratigraphy of the Exmouth Plateau archives are: (i) dominated by bottom-current deposits and associated erosional features from the Late Cretaceous to Late Miocene; and (ii) dominated by the emplacement of MTCs since the Late Miocene. The former is linked to rifting and the opening of ocean gateway along the southern margin of the continent, and the latter is related to a collision and the closing of ocean gateway along the northern margin of the continent.

2. Geological setting

2.1 Tectonostratigraphic framework

The Exmouth Plateau is located between upper and lower slopes of the northwest Australia continental margin (Falvey & Veevers, 1974), in water depths ranging from 800 to 4000 m (Exon *et al.*, 1992). The plateau is bound by continental shelf to the southeast, and the Argo, Gascoyne and Cuvier abyssal plains to the northeast, northwest and southwest, respectively (Longley *et al.*, 2002) (Fig. 1). The Exmouth Plateau is a sub-basin of the North Carnarvon Basin, which underwent at least two rifting events (Tindale *et al.*, 1998; Longley *et al.*, 2002) in the Triassic and Early Cretaceous forming the three abyssal plains (Fig. 1).

This study focuses on the late post-rift megasequence (Fig. 2), which is Late Cretaceous to Recent in age, and is defined, on the Exmouth Plateau at least, by the sustained deposition of fine-grained carbonates (i.e. chalk and oozes) as recorded in ODP 762 and 763 cores (Figs 2 and 3) (Haq *et al.*, 1992; Boyd *et al.*, 1993). An unconformity defining the Cretaceous-Palaeogene boundary (Boyd *et al.*, 1993) most probably formed by enhanced bottom-current erosion (Fig. 2) (Haq *et al.*, 1992) related to the change of primary seafloor spreading axis from the Indian to the Southern Ocean (Fig. 2) (Baillie *et al.*, 1994). At the start of the Oligocene, a global eustatic sea level fall occurred as a result of continental ice sheet build-up in Antarctica (Miller *et al.*, 1991). Oligocene to Late Miocene sediments are the thickest beneath the present shelf where they are represented by a progradational, clinoform-bearing carbonate succession; further basinward, on the Exmouth Plateau, this interval is represented by a thin pelagic succession (Tindale *et al.*, 1998). Another unconformity defining the base of the Late Miocene to Recent succession most probably record collision between Australia and Eurasia (Boyd *et al.*, 1993). The Late Miocene to Recent succession thickens further basinward and onlaps the underlying sediments on the shelf (Fig. 4), suggesting accelerated tectonic subsidence on the Exmouth Plateau associated with inverted pre-existing faults beneath the present shelf (Fig. 2) (Hull & Griffiths, 2002). The collision is variably expressed along the

Northwest Shelf of Australia (e.g. the Exmouth Plateau Arch), which is controlled by the orientation between the regional compressional stress field and pre-existing, rift-related structures (Keep *et al.*, 1998). On the Exmouth Plateau, broad folding of the Exmouth Plateau Arch about an NE-SW axis led to gravity-driven deposition resulting to MTCs deposition, with sediments being thin on the plateau crest and thick in the adjacent Kangaroo Syncline (see Fig. 3) (Boyd *et al.*, 1993).

2.2 Present-day oceanographic setting

Two currents dominate the present-day ocean circulation offshore NW Australia (Fig. 1) (e.g. Wells & Wells, 1994): (i) the poleward-flowing Leeuwin Current and (ii) the equatorward-flowing Western Australian Current (WAC) (Fig. 1). Most ocean basins in the southern hemisphere are dominated by an anti-clockwise gyre, which results in an Eastern Boundary Current that flows northward to the equator along continental margins (e.g. Benguela Current, offshore southern Africa, and the Humboldt Current, offshore Peru and Chile) (Collins *et al.*, 2014). The Northwest Shelf of Australia is dominated by the southward-flowing Leeuwin Current rather than the Eastern Boundary Current (i.e. the WAC) (Fig. 1). The Leeuwin Current is a low-salinity, nutrient-poor, narrow (<100 km wide), high velocity current (0.1 to 0.4 m/s), flowing down to 300 m water depth (James *et al.*, 2004). It is sufficiently energetic (Pearce, 1991) to form depositional bedforms within sand-sized sediments (Stow *et al.*, 2009). The LC flows as a result of strong trade winds in the equator that push the westward-flowing South Equatorial Current (SEC) through Indonesia (Fig. 1) (Collins *et al.*, 2014). The SEC induces a pressure-gradient in the eastern Indian Ocean that forces warm surface water to flow southward along the western shelf of Australia, i.e. the Leeuwin Current (Smith *et al.*, 1991). The other current, the WAC (Fig. 1), is a cold, high-salinity, nutrient-rich current (Spooner *et al.*, 2011), which influences water masses as deep as 2000 m (Tchernia, 1980).

3. Data set and methodology

3.1 Data set

We use two types of seismic reflection data (see Fig. 3 and Table S1), provided by Geoscience Australia: (i) 412 2D data lines with a cumulative line length of ~40,000 km, and which cover an area of ~109,000 km^2. These data were collected between 1993 and 2005, with the dominant frequency ranging from 30 to 50 Hz in the interval of interest, and (ii) a 3D seismic volume (Duyfken 3D MSS, acquired in 2006) that covers an area of 3627 km^2, with a bin size of 18.75 x 12.5 m (i.e. inline x crossline) and a dominant frequency of 50 Hz in the interval of interest (Fig. 3). Given an average velocity of 2000 m/s derived from checkshot data from wells, we estimate the vertical resolution ($\lambda/4$) of the seismic data ranges from 10 – 17 m for the 2D data, and is c. 10 m for the 3D data. Seismic reflection data polarity follows SEG normal convention (Brown, 2011), where a downward increase of acoustic impedance manifests as a negative reflection event (trough), and a downward decrease of acoustic impedance manifests as a positive reflection event (peak).

This study uses 12 wells that provide lithological and well-log (Table S2 and S3), biostratigraphic (Table S4 and Fig. S1), palaeo-water depth (Fig. S2 and S3), and velocity (Fig. S4) data within the study interval. These wells are chosen based on their spatial distribution (i.e. in an area where several wells are clustered, only the well with the most complete data was chosen). The study interval is not a primary petroleum exploration target, therefore borehole data (e.g. lithological, biostratigraphic, and well-log) is rather sparse (see Tables S2-S4 and Figs S1-S2). Industry wells provide lithology data based on ditch cuttings, with conventional core data provided by two ODP Leg 122 wells (ODP 762 and 763). Most well-logs terminate below or within the lower part of the study interval, and only GR (gamma-ray) logs sample the majority of the study interval. Of the 12 wells, five contain biostratigraphic data within the study interval. These wells were utilised to constrain the age of interpreted surfaces from seismic reflection data, and biostratigraphic data provided palaeo-water depth estimations (Fig. S2). However, because palaeo-water depth data are scarce in the upper part of the study interval, we infer the palaeo-water depth based on the height of Oligocene to Recent clinoforms (see Hull & Griffiths, 2002) (Fig. 2). Velocity data were used to convert seismic interpretation deliverables (e.g. time-structure maps) from the time domain in milliseconds two-way time (ms TWT) to the depth domain in meters by using 2nd-order polynomial best-fit line equation (Fig. S4).

3.2 Methodology

3.2.1 Seismic-stratigraphic framework

Exon and Willcox (1980) conducted the earliest seismic reflection-based investigations of the Exmouth Plateau. Following drilling of ODP Leg 122 wells (i.e. ODP 762 and 763), Boyd *et al.* (1993) updated previous interpretations, providing better lithology and age constraints on the penetrated succession. Our study recognises four regionally significant horizons (Figs 2 and 4) previously identified by Boyd *et al.* (1993). These horizons were interpreted based on seismic-stratigraphic relationships (i.e. truncation, onlap, and downlap), and vertical and lateral variations of internal seismic reflection geometry. The interpreted horizons, i.e. Horizon A, B, C, and D, define three seismic units (Figs 2 and 4): (i) SU-1 – Late Cretaceous, equivalent to Package 6 of Boyd *et al.* (1993); (ii) SU-2 – Palaeocene-Late Miocene, equivalent to Package 7 of Boyd *et al.* (1993); and (iii) SU-3 – Late Miocene-Recent, equivalent to Package 8 of Boyd *et al.* (1993). We mapped five additional horizons within SU-2 within the 3D seismic dataset; these relatively high-amplitude, continuous seismic reflections horizons, which are only locally mappable, define vertical changes in seismic facies and, we infer, depositional locus and process. However, only three of them (i.e. Horizon C-2, C-3, and C-4) are discussed further here (Section 4.2), as they provide the most significant evidence to interpret palaeo-oceanographic processes. Seismic attributes, such as RMS amplitude and variance (see Text S1 for explanation), were extracted from the 3D seismic reflection data to aid interpretation and to augment conventional seismic mapping (Brown, 2011).

3.2.2 Borehole data interpretation

Several wells provide lithologic control on the studied succession. ODP 762 and 763 wells contain conventional core throughout the study interval, with other wells yielding ditch cuttings (Table S2). Figure 5 illustrates the well-log coverage and lithology distribution within the study interval from the outer shelf (east) to the basin (west). The age of seismic surfaces are constrained by biostratigraphic data (Table S4 and Fig. S1); in this study we used a planktonic foraminifera-based biozonation scheme, as the associated data are consistently available in all five wells containing biostratigraphic data. In addition, palaeo-water depth, derived from several wells (Fig. S2), we also incorporated in our analysis. Note that we refer to biozonation scheme of Kelman *et al.* (2013) and the geological timescale of Gradstein *et al.* (2012).

4. Results

We identified three seismic units (SUs) within the studied interval (SU-1-3). These SUs are bound by four regional surfaces (A-D, from oldest to youngest), with D representing the seabed (see Fig. 4). In this section we describe and interpret the composition and age (Fig. 5), and the internal (i.e. internal seismic facies and thickness variations) and external (i.e. basal surface geometry) characteristics of each SU (Fig. 6).

4.1 SU-1 (Late Cretaceous)

SU-1 is bound by Horizon A and B at the base and top, respectively. SU-1 is composed of carbonate-dominated sediments (i.e. marl and chalk), which overlie clay-dominated, siliciclastic sediments (Fig. 5). Horizon A therefore marks the transition from a clastic- to carbonate-dominated depositional regime. Biostratigraphic data (Fig. S1) show that the Horizon A defines the Cenomanian/Turonian boundary.

4.1.1 Basal surface: Horizon A

Horizon A defines the base of the studied interval. It truncates underlying seismic reflections, especially along the axis of the Kangaroo Syncline axis (e.g. Figs 7a and c); elsewhere, it is generally conformable (e.g. Figs 7f and h).

Two elongate, at least 7.5 km-long and 3 km-wide sedimentary bodies, oriented sub-parallel to the present, NE-trending slope are observed on Horizon A ('pre-SU-1 mounds'; outlined in red in Fig. 8b). These bodies are defined by sub-parallel, continuous, reflections in their lower part, and are mounded in their upper part (Figs 7a, c-d).

The 3D seismic data imaged one of the pre-SU-1 mounds, where Horizon A displays significant relief of at least 500 m (Figs 7a and 9a). An RMS amplitude map of Horizon A reveals a suite of predominantly NE-trending amplitude anomalies (Fig. 9b). These anomalies are: (i) sinuous lineations corresponding to truncation of underlying reflections (Fig. 9c), and (ii) straight lineations defining U-shaped depressions (c. 2.5 km-wide and c. 100 m-deep) (Fig. 9d).

4.1.2 Characteristics of SU-1

Due to erosion along Horizon B, SU-1 varies in thickness (e.g. Figs 7b-d). Major (up to 500 m thick) SU-1 depocentres are located along the Kangaroo Syncline, where they are c. 200 km-long and 70 km-wide, and trend NE, sub-parallel to the present slope (Fig. 8c). Between these elongate depocenters, SU-1 is relatively thin and has a channel-like form (Figs 7b-c) shaped by Horizon B, that incises down up to 250 m. Elsewhere, such as in the northern and western part of the study area, SU-1 has a broadly uniform thickness (c. 250 m), progressively thinning southward (Fig. 7e) and westward (Fig. 7f).

Although SU-1 is dominated by SF-1 (Figs 7b and 8c), internal seismic facies variations occur. For example, a NE-trending, channel-like seismic facies (i.e. SF-2, see Fig. 6) occur along the Kangaroo

Syncline (Figs 7b-c and 8c). The 3D seismic data partly imaged this features, showing it corresponds to the sinuous lineations (Figs 9a-c) described above.

4.1.3 Interpretation of SU-1

Beneath Horizon A, a progressive change of seismic facies within the pre-SU-1 mounds, from sub-horizontal in the lower part to more mounded upwards (Figs 7a and c-d), resembles a classic mounded drift development (e.g. Faugères *et al.*, 1999). The truncation of reflections at the top of the pre-SU-1 mounds by Horizon A (Figs 7a and c-d) indicate a major erosional event following construction of the mounded drifts. We therefore interpret both constructional and erosional processes controlled development of pre-SU-1 mounds. In addition, their elongate geometry, in particular their orientation sub-parallel to the NE-trending present slope (Fig. 8b), is consistent with an origin as contourite drifts (e.g. Rebesco *et al.*, 2014).

SU-1 was deposited in relatively deep-marine (>200 m), an interpretation supported by palaeo-water depth data from: (i) wells (Fig. S4), which indicate at least upper neritic to bathyal depths (100-500 m); (ii) biostratigraphic data from Hull and Griffiths (2002), which indicate water depths of 200-1000 m in Rankin Platform and Dampier Sub-basin (Fig. 3); and (iii) Boyd *et al.* (1993), who suggest that, based on the topographic relief of the Pre-SU-1 interval (their Package 5), suggest the palaeo-water depth at this time was at least 300 m.

Pelagic or hemipelagic deposition dominated during deposition SU-1 (i.e. SF-1; e.g. Figs 7b-c and e). An alternative interpretation, based on their tabular-to-low-relief mounded geometries, and their mid-slope position, is these seismic packages represent slope sheeted drifts (Faugères *et al.*, 1999; Hernández-Molina *et al.*, 2008). The 3D seismic reflection data image evidences of contour current activities: (i) the sinuous lineations interpreted as contourite channel (Figs 8c and 9b-c); and (ii) straight lineations interpreted as erosional remnants (Figs 9b and d). We did not interpret the latter as gullies (cf. Lonergan *et al.*, 2013), because these features are: (i) normal rather than parallel to the slope; (ii) significantly larger (as compared to gullies in that study, which are only 160-625 m-wide and 8-43 m-deep), and (iii) not regularly-spaced.

4.2 SU-2 (Early Palaeocene-Late Miocene)

SU-2 is bound by Horizon B and C at the base and top, respectively. SU-2 is composed of calcarenite and calcilutite along the NW Shelf, and pelagic chalk further north-westward on the Exmouth Plateau Arch (Fig. 5). Biostratigraphic data (Fig. S1) show that the Horizon B defines Cretaceous/Palaeogene boundary (cf. Reflector 6 of Boyd *et al.* (1993).

4.2.1 Basal surface: Horizon B

Horizon B can be traced across much of the study area. It is generally characterised by a high-amplitude, continuous, negative reflection that is commonly offset by low-displacement normal faults (e.g. Fig. 7b). As previously discussed, Horizon B truncates SU-1, defining the prominent SU-2 contourite channel (Figs 8c-d). Highly irregular relief (c. 200 m) produced by this horizon is located within an area termed as the 'V-shaped facies zone' (VFZ) (Figs 7d and 8d); this is discussed in detail later in this section.

4.2.2 Characteristics of SU-2

Thickness patterns in SU-2 defines a marked shift in the locus of deposition (Fig. 8e), most notably around the Exmouth Plateau Arch. Here, SU-2 thins south-westward (from 500 m to 200 m, Fig. 7e) and thickens (c. 450 m) westward (Fig. 7f); this contrasts with SU-1, which was progressively thinning westward.

SU-2 contains three distinctive seismic facies (see Fig. 8d): (i) SF-1 dominates (e.g. Figs 7e and h), with sub-horizontal and NE-dipping variants observed (Fig. 7a); (ii) SF-2, which is best-developed found along the axis of the SU-2 contourite channel (Figs 7b-c); and (iii) SF-3, which is best-developed within the VFZ, and is imaged in the NE of the 3D dataset (Figs 7a, d and 8d). The detailed geometry of the VFZ is difficult to interpret in 2D seismic reflection data due to the relatively low resolution of these data, and the inherent stratigraphic complexities of this part of SU-2 (see Horizon C-4 in Fig. 7d). We therefore used three horizons (i.e. C-2 to C-4) mapped in the 3D seismic reflection data that allow us to better understand the transition from an area where relatively simple, NE-dipping reflections of SF-1, to the more complex VFZ (e.g. Figs 7a and 8d).

The interval between B and C-1 is dominated by sub-parallel reflections that are offset by low-displacement normal faults (SF-1) (Fig. 10a). The overlying interval (C-1 to C-2) is composed of continuous wavy reflections above the pre-SU-1 mound slope, changing laterally into discontinuous but locally wavy reflections to the NE (Fig. 10a). The wavy reflections along C-2 have a maximum amplitude of 40 m, with the wavelength between two troughs being up to 3 km. Wave crests trend NNW and can be traced for up to ~12 km (Fig. 10b). Between C-2 and C-3, the wave crests migrate south-westward by ~1 km (Fig. 10a-c), with wave amplitude and wavelength on C-3 being similar to that on C-2. However, C-3 truncates C-2 above the pre-SU-1 mound at the base-of-slope (Fig. 10a), forming predominantly ENE-trending scours on the NW and SE sides of the waves (Fig. 10c). Between C-3 and C-4, waves migrate a further c. 500 m to the SW (Figs 10a, c-d), with local preservation of the 4 km wide, 100 m deep scours previously formed along Horizon C-3 (Fig. 10d). Lineations up to 10 km-long, 5-20 m-deep, and 60-150 m-wide occur on the base of scours developed along C-4 (Fig. 10d). The interval between C-4 and C is predominantly composed of sub-parallel reflections, with an erosional surface (C-5) in between.

4.2.3 Interpretation of SU-2

Biostratigraphic data from Orhtrus-1 indicate the palaeo-water depth at the beginning of SU-2 deposition was at least 200 m (Fig. 3). In addition, Hull and Griffiths (2002) suggest the palaeo-water depth was at least 300 m and progressively increased to 600 m during Early Oligocene (Rupelian), based on average clinoform heights in the Dampier Sub-basin (Figs 3 and 4). Together, these data imply that SU-2 deposition was deeper than that of SU-1.

Thickness variations in SU-2 reflect growth of the Exmouth Plateau Arch. Folding of the arch may have occurred after deposition of SU-2, an interpretation supported by truncation of reflections within SU-2 by Horizon C (Figs 7f-g), and the apparent lack of true depositional thinning onto the arch crest. In this case, thickness changes in SU-2 are primarily driven by erosion at its top, with this being greatest near the arch crest.

Although SU-2 is dominated by pelagic and hemipelagic deposition (SF-1), bottom current activity is evident by the SU-2 contourite channel and additional erosional features within the VFZ (Fig. 8d). SU-2 filled accommodation created by Horizon B, suggesting bottom current strength decreased with time (e.g. Faugères & Stow, 2008).

The NE-dipping reflections (Fig. 7a) are interpreted to be down-current migrating (to the NE), slope sheeted contourite drift (Faugères *et al.*, 1999) (Fig. 7c). This drifts passes north-eastward into large (sensu Symons *et al.*, 2016; Hofstra *et al.*, 2018), fine-grained (sensu Wynn & Stow, 2002) sediment waves that define the VFZ. We suggest these sediment waves formed in response to bottom current activity, as opposed to turbidity currents, because of their close temporal and spatial relationship with the sheeted contourite drift. Sediment waves continued to grow and migrate to the SW up to C-4 (Fig. 10a). We infer bottom current flowed NE-ENE, as bottom current direction is generally perpendicular (Flood, 1988) or oblique (Blumsack & Weatherly, 1989) to sediment wave crests (Fig. 10b).

The geometry of erosional features (i.e. scours) first developed at C-3, which continue up to C-4, imply the sediment waves became an obstacle to bottom current flow, resulting in flow separation and subsequent erosion on the marginal sides of the obstacle (e.g. Hernández-Molina *et al.*, 2006a). In addition, on the down-current side of the large sediment waves, depositional 'tails' developed as a result of complex flow interactions and decreasing flow velocities behind the obstacle (Figs 10c-d) (Davies & Laughton, 1972; Hernández-Molina *et al.*, 2006a). These tails were expressed as discontinuous wavy reflections (Fig. 10a). In addition, lineations at the base of the scours have morphology and dimensions that are consistent with an interpretation as furrows (Stow *et al.*, 2009).

We suggest the depositional and erosional features interpreted here reflect activity of the equatorward-flowing, 'palaeo'-WAC (i.e. Palaeocene to Oligocene). Evidence for deep-time activity of the WAC is rare. One example is provided by Cathro *et al.* (2003) in the Dampier Sub-basin (Fig. 3), where they observe northeastward progradation of late Middle Miocene foresets, which was normal to the northwestward progradation of the continental margin.

An alternative interpretation of the VFZ is provided by Imbert and Ho (2012), who studied this zone in more detail. They interpret the V-shaped features as fossil hydrate pockmarks (i.e. collapsed pockmarks) initiated by methane hydrate emplacement along conical failures originating from the subsurface to Palaeocene-Eocene seabed. The emplaced methane hydrate was then dissociated, driving formation of collapsed pockmarks. Although this model may locally apply in the more stratigraphically complex middle part of the VFZ (Fig. 8d), it does not consider the strong evidence for bottom current activity we document immediately adjacent to the VFZ. Instead, they suggest this zone documents an area where large volumes of near-surface sediment were remobilised and expelled due to gas migration. Although plausible, we argue this hypothesis is not supported by any substantial evidence for the presence of gas hydrate (e.g. bottom simulating reflector in seismic reflection data). Nevertheless, irrespective of the exact origin of the V-shaped features within the VFZ, it is evident that bottom current activity played an important role in SU-2 deposition.

4.3 SU-3 (Late Miocene-Recent)

SU-3 is bound by Horizon C and D (seabed) at the base and top, respectively. The composition of the SU-3 is similar to that of SU-2 (i.e. calcarenite and calcilutite on the shelf and chalk on the plateau), although cores from ODP 762 and 763 indicate calcareous oozes dominate around the Exmouth Plateau Arch. Biostratigraphic data (Fig. S1) show that Horizon C defines an unconformity between the Middle and Late Miocene, equivalent to Reflector 7 of Boyd *et al.* (1993) and N17-1 horizon of Hull and Griffiths (2002).

4.3.1 Basal surface: Horizon C

Horizon C is a low- to high-amplitude, relatively continuous reflection. In places, especially along the Kangaroo Syncline and on the flanks of the Exmouth Plateau Arch, it underlies chaotic seismic reflections (SF-4) (Figs 7a, d, and h).

4.3.2 Characteristics of SU-3

SU-3 is mainly contained in a depocentre in the NE-part of the study area, where it is up to 1000 m thick. The unit is thinnest (c. 50 m) across the Exmouth Plateau Arch (Fig. 8e). SU-3 contains two dominant seismic facies (Fig. 8e): (i) SF-1, which is widespread across the study area (e.g. Figs 7c-d); and (ii) SF-4, which dominates in the present-day topographic lows, such as along the Kangaroo Syncline (Figs 7a, d, and h), and the western and southern flanks of the Exmouth Plateau Arch (Fig. 7g).

The 3D seismic reflection data partly imaged an area where SU-3 is dominated by stacked packages of SF-4 (Fig. 11a). Locally, two horizons are mapped in the area (D-1-2), bounding at least three packages of SF-4 (MTC-1-3) (Fig. 11a). Within these package we observe (Figs 11b-d): (i) 1-5 km wide blocks of more coherent reflections and lateral margins (up to 200 m-deep) of MTC-1, between Horizon C and D-1 (Figs 11a-b); (ii) up to 20 km-long erosional grooves that are best-expressed along D-1 at the base of MTC-2 (Figs 11a and c); and (iii) primary and secondary flow fabrics (PFFs and SFFs) with relief of ~30 m and lateral margin (~140 m-deep) of MTC-3 expressed at the top surface of MTC-3 (Horizon D) (Figs 11a and d), from which MTC-3 can be divided into MTC-3 a and b. All of these kinematic indicators are generally NW-trending, approximately the same with the trend of the sediment wave crestlines within SU-2 (Figs 10b-d).

4.3.3 Interpretation of SU-3

Biostratigraphic data indicate that, since the Middle Miocene, water depth in the Exmouth Plateau was generally bathyal (Fig. S4), with clinoforms height in the Dampier Sub-basin suggesting water depths of at least 800 m based (Fig. 2) (Hull & Griffiths, 2002). Therefore, SU-3 deposition was significantly deeper than the previous SUs.

Thickness patterns of SU-3 suggest further growth of the Exmouth Plateau Arch during this time, although a mismatch between the arch crest and the thinnest succession suggests that the uplift occurred after the deposition of SU-3. Coeval with the arch growth, deposition during SU-3 times (Figs 7a, d, and 8e) was dominated by the emplacement of mass-transport complexes (MTCs). Horizon C, which underlies these chaotic facies in many places, is therefore interpreted as a basal shear surface (BSS), along which materials were transported and deposited (Bull *et al.*, 2009). Elsewhere, pelagic and hemipelagic deposition occur (Fig. 8e).

The MTCs were predominantly deposited in present-day topographic lows (Fig. 8e), such as along the Kangaroo Syncline (Figs 7a, d, and h) and on the flanks of the Exmouth Plateau Arch (Fig. 7g). In the Kangaroo Syncline, several MTCs were deposited (Figs 7a, d, and h). Based on headwall scarp trends on the seabed (Fig. 8e), and kinematic indicators within them (e.g. lateral margin and groove orientations), these stacked MTCs were derived from either the arch and transported landward, or from the NW shelf and transported seaward. The youngest MTCs originated from the shelf (i.e. MTC-3 in Fig. 11a) have an estimated volume between 50 to 100 km^3 (Hengesh *et al.*, 2013).

5. Discussion

We have shown that Late Cretaceous to Late Miocene deposition on the Exmouth Plateau was dominated by slope-parallel bottom currents (producing contourite drifts and channels), whereas post-Miocene deposition was dominated by down-slope, gravity-driven processes (mainly manifested as MTC deposits). In this section, we discuss the significance of this change in dominant process regime, in particular how this may correlate with regional tectonics and palaeo-oceanographic events that were occurring simultaneously along the southern and northern margins of Australia.

5.1 Palaeo-oceanographic evolution of the NW Australia continental margin

A period of major tectonic plate reorganisation occurred in the Cenomanian (Powell *et al.*, 1988; Veevers *et al.*, 1991). Oceanic crust was generated as a result of seafloor spreading between Australia and Antarctica (Fig. 12a) (Baillie *et al.*, 1994), with the deep-ocean connecting western Australia to the Pacific Ocean forming in the Oligocene. This implies that the circum-polar current around Antarctica was deflected onto the western margin of Australia from the Cretaceous until the late Palaeogene (Baillie *et al.*, 1994). The widespread base Turonian erosional surface (i.e. Horizon A) on the Exmouth Plateau may record initiation of this circum-polar current, herein interpreted as the 'proto'-WAC. However, contourite deposition on the Exmouth Plateau may have initiated before the Turonian (~93 Ma) (i.e. sub-Horizon A), as evidenced by the development of a pre-SU-1 mounded drift (e.g. Fig. 7a).

After a ~27 Myr period of bottom current activity and contourite deposition, another major erosional event occurred at the end Cretaceous (~66 Ma) (Horizon B). This event coincides with the change of the primary ocean spreading axis from the Indian Ocean to the Southern Ocean (Powell *et al.*, 1988) (Fig. 12b), which marked initial opening of the major ocean gateway between Australia and Antarctica. By the Early Oligocene, this gateway was open, and circum-polar ocean current circulation around Antarctica was fully established (Fig. 12c) (Miller *et al.*, 1991). The establishment of circum-polar circulation and genetically-related continental ice sheet build-up on Antarctica led to a global sea level fall (Miller *et al.*, 1991). We suggest that a deepening of bottom current activity due to a eustatic sea-level fall, combined with a strengthening of the associated proto-WAC, is recorded on the Exmouth Plateau by the growth of contourite sheeted drift and sediment waves, and the development of deep scours, especially in the transition zone into the VFZ (Fig. 10). The Quaternary record supports this interpretation, with the WAC being stronger than the Leeuwin Current during glacial periods (Spooner *et al.*, 2011).

During SU-3 deposition, bottom current activity might have been masked by down-slope depositional processes dominated by deposition of MTCs. We attribute this change in depositional style to reflect increased tectonic activity along the northern margin of Australia, related to the collision between the northward-moving Australian Plate, and the Pacific and Eurasia plates, which began in the Early Miocene (Fig. 12d) (Boyd *et al.*, 1993; Baillie *et al.*, 1994). However, bottom current-related deposits are observed on the late Middle Miocene succession preserved in the Dampier Sub-basin, as documented by (Cathro *et al.*, 2003). Present-day, bottom current features (e.g. furrows) are still observed on the seabed (Day *et al.*, 2010). This implies that the WAC is still influencing the seabed on the >800 m deep plateau, rather than the LC, which only operates down to relatively shallow water depths (maximum 300 m) (Fig. 4).

By using seismic reflection data, we are able to show that the Late Cretaceous to Recent succession offshore NW Australia archives two major events that impacted global thermohaline ocean circulation, with the Exmouth Plateau uniquely located between oceanic gateways that were either opening (i.e. Tasman Gap) or closing (i.e. Indonesian Seaway) during deposition (Knutz, 2008). In contrast, few studies have used seismic reflection data to document pre-Quaternary bottom current activity and related deposits (Romine *et al.*, 1997; Cathro *et al.*, 2003). This also advances palaeo-oceanographic understanding offshore Western Australia. Previous studies have been conducted using various proxies, such as Mg/Ca ratio, carbon and oxygen isotopes, and foraminifera assemblages (Wells & Wells, 1994; Sinha *et al.*, 2006; Murgese & De Deckker, 2007; Karas *et al.*, 2011; Spooner *et al.*, 2011), but have only extended palaeo-oceanographic history to the Early Pleistocene (2.2 Ma) (Sinha *et al.*, 2006).

5.2 Triggering mechanisms of mass-transport complexes (MTCs) emplacement

Slope failure occurs when the shear strength of a sediment (or material) is exceeded by the shear stress required for equilibrium (Hampton *et al.*, 1996; Duncan & Wright, 2005). Therefore, slope failure can occur due to (1) shear stress increases (e.g. due to an earthquake-related seismic shaking), (ii) slope oversteepening (e.g. related to increased sediment influx or to tectonics), and/or (iii) shear strength decreases (e.g. due to fluid expulsion, gas hydrate dissociation, and/or high sedimentation rates) (e.g. Hampton *et al.*, 1996; Locat & Lee, 2002).

Bottom simulating reflectors (BSRs), indicative of gas hydrates (e.g. Hyndman & Spence, 1992), are absent within the study area (Scarselli *et al.*, 2013). Furthermore, Neogene sedimentation rates on the Exmouth Plateau are relatively low (20 mMa^{-1}) (Golovchenko *et al.*, 1992). This is 40 times lower than many basins that become overpressured due to high sediment accumulation rates, such as in Tertiary delta provinces (e.g. Osborne & Swarbrick, 1997). Gas hydrate dissociation and high sedimentation rates are therefore not considered as triggering mechanisms for MTCs emplacement in the study area.

In contrast, seismic shaking due to earthquakes, tectonically-related slope oversteepening and fluid expulsion are the most likely triggers for MTCs emplacement on the Exmouth Plateau. Tectonic reactivation of pre-existing structures along the NW Shelf of Australia, possibly related to plate collision along the northern margin, could have induced slope oversteepening in concert with increased seismicity (Keep *et al.*, 1998). Tectonically-related arching of the NE-trending Exmouth Plateau Arch probably led to the deposition of MTCs from the arch crest to the east (landward) and west (seaward) (Boyd *et al.*, 1993; Hengesh *et al.*, 2013; Scarselli *et al.*, 2013). Subsurface fluid migration and trapping in impermeable layers may have also 'primed' the slope to fail, although seabed pockmarks provide some evidence for fluid venting (Hengesh *et al.*, 2013).

6. Conclusions

We integrate of 2D and 3D seismic reflection and borehole data to define three seismic units (SUs) within the overall deep-marine, fine-grained, carbonate-dominated Exmouth Plateau, offshore NW Australia. In the Late Cretaceous (palaeo-water depth of c. 200 m), bottom currents are manifested by a range of contructional bedforms (e.g. controurite drift) and erosional features (e.g. contourite channel). These features result from strong bottom-currents, which are inferred to have been the ancient equivalents of the major oceanic circulation system seen in the modern Indian and Southern oceans. During this time, the circum-polar ocean current, which circulates around the Antarctica in the present-day Southern Ocean, was deflected along the western margin of Australia. We interpret this circum-polar ocean current as the 'proto'-West Australian Current (WAC). Ongoing bottom current activity during the Palaeocene to Oligocene in water depths of c. 200-600 m is expressed by large sediment waves and related scours. These features were formed by NE-flowing bottom currents, interpreted as the proto-WAC, which intensified during a glacial period following the establishment of circum-polar ocean circulation around Antarctica. In the Late Miocene to Recent (palaeo-water depth of c. 800 m), large (up to 100 km3) abundant mass-transport complexes (MTCs) were sourced from the continental margin to the SE, or the Exmouth Plateau Arch to the NW. At this time, the Exmouth Plateau lay in deeper water and lacked evidence for bottom-current activity. Tectonically-induced oversteepening of the continental margin and intra-basin Exmouth Plateau Arch, linked to ongoing collision along the northern margin of the Australia plate, was the most likely triggering mechanism for deposition of the MTCs. Hence, the stratigraphy of the Exmouth Plateau records two regional geological events related to (i) earlier rifting and the opening of an ocean gateway along the southern margin of the continent, and (ii) later collision and associated closure of an ocean gateway along the northern margin of the continent. The Exmouth Plateau stratigraphy is a valuable archive of plate tectonically-driven changes in palaeo-oceanographic currents, which can be applied to areas and time periods with sparser data coverage.

7. Acknowledgements

We thank Geoscience Australia for providing seismic and borehole data, IODP for providing ODP wells, and Schlumberger for providing software. The first author thanks the Indonesia Endowment Fund for Education (LPDP) (Grant No.: 20160822019161) for its financial support. Thank you to Michael Steventon and Nan Wu for their valuable suggestions to improve the manuscript.

8. Conflict of Interest

No conflict of interest declared.

9. References

AKHURST, M.C., STOW, D.A. & STOKER, M.S. (2002) Late Quaternary Glacigenic Contourite, Debris Flow and Turbidite Process Interaction in the Faroe-Shetland Channel, NW European Continental Margin. *Geological Society, London, Memoirs*, **22,** 73-84

ALFARO, E. & HOLZ, M. (2014) Seismic Geomorphological Analysis of Deepwater Gravity-Driven Deposits on a Slope System of the Southern Colombian Caribbean Margin. *Marine and Petroleum Geology*, **57,** 294-311

ARMANDITA, C., MORLEY, C.K. & ROWELL, P. (2015) Origin, Structural Geometry, and Development of a Giant Coherent Slide: The South Makassar Strait Mass Transport Complex. *Geosphere*, **11,** 376-403

BAILLIE, P., POWELL, C.M., LI, Z. & RYALL, A. (1994). *The Tectonic Framework of Western Australia's Neoproterozoic to Recent Sedimentary Basins*. The Sedimentary Basins of Western Australia: Proceedings of Petroleum Exploration Society of Australia Symposium.

BLUMSACK, S. & WEATHERLY, G. (1989) Observations of the Nearby Flow and a Model for the Growth of Mudwaves. *Deep Sea Research Part A. Oceanographic Research Papers*, **36,** 1327-1339

BOYD, R., WILLIAMSON, P. & HAQ, B. (1993) Seismic Stratigraphy and Passive-Margin Evolution of the Southern Exmouth Plateau. In: *Sequence Stratigraphy and Facies Associations* (Ed. by H. W. Posamentier, C. P. Summerhayes, B. U. Haq & G. P. Allen), **18**, 579-603. Blackwell Scientific Publications, Oxford.

BROWN, A.R. (2011) *Interpretation of Three-Dimensional Seismic Data*. The American Association of Petroleum Geologists and the Society of Exploration Geophysicists, Tulsa.

BULL, S., CARTWRIGHT, J. & HUUSE, M. (2009) A Review of Kinematic Indicators from Mass-Transport Complexes Using 3d Seismic Data. *Marine and Petroleum Geology*, **26,** 1132-1151

CAMPBELL, D. & DEPTUCK, M. (2012) Alternating Bottom-Current-Dominated and Gravity-Flow-Dominated Deposition in a Lower Slope and Rise Setting—Insights from the Seismic Geomorphology of the Western Scotian Margin, Eastern Canada. *Application of the Principles of Seismic Geomorphology to Continental-slope and Base-of-slope Systems: Case Studies from Seafloor and Near-seafloor Analogues. SEPM Special Publication*, **99,** 329-346

CATHRO, D.L., AUSTIN JR, J.A. & MOSS, G.D. (2003) Progradation Along a Deeply Submerged Oligocenemiocene Heterozoan Carbonate Shelf: How Sensitive Are Clinoforms to Sea Level Variations? *AAPG bulletin*, **87,** 1547-1574

CATHRO, D.L. & KARNER, G.D. (2006) Cretaceous–Tertiary Inversion History of the Dampier Sub-Basin, Northwest Australia: Insights from Quantitative Basin Modelling. *Marine and Petroleum Geology*, **23,** 503-526

CLARK, I., CARTWRIGHT, J., PRATHER, B., DEPTUCK, M., MOHRIG, D., VAN HOORN, B. & WYNN, R. (2012) Interactions between Coeval Sedimentation and Deformation from the Niger Delta Deepwater Fold Belt. In: *Application of the Principles Seismic Geomorphology to Continental Slope and Base-of-Slope Systems: Case Studies from Seafloor and near-Seafloor Analogues*

(Ed. by B. Prather, M. E. Deptuck, D. Mohrig, B. V. Hoorn & R. Wynn), *Sepm Special Publication*, **99**, 243-267. SEPM (Society for Sedimentary Geology).

Collins, L.B., James, N.P. & Bone, Y. (2014) Carbonate Shelf Sediments of the Western Continental Margin of Australia. *Geological Society, London, Memoirs*, **41,** 255-272

Davies, T. & Laughton, A. (1972) Sedimentary Processes in the North Atlantic. *Initial reports of the deep sea drilling project*, **12,** 905-934

Day, K., Gale, J. & Smallwood, J. (2010) Deepwater Exmouth Plateau, North Carnarvon Basin: Preliminary Investigations into Ridge and Furrow Features. *APPEA*, **50,** 731-731

Duncan, J. & Wright, S. (2005) Soil Strength and Slope Stability, John Wiley & Sons Ltd

Ercilla, G., Juan, C., Hernandez-Molina, F.J., Bruno, M., Estrada, F., Alonso, B., Casas, D., Lí Farran, M., Llave, E. & Garcia, M. (2016) Significance of Bottom Currents in Deep-Sea Morphodynamics: An Example from the Alboran Sea. *Marine Geology*, **378,** 157-170

Esmerode, E.V., Lykke-Andersen, H. & Surlyk, F. (2008) Interaction between Bottom Currents and Slope Failure in the Late Cretaceous of the Southern Danish Central Graben, North Sea. *Journal of the Geological Society*, **165,** 55-72

Exon, N., Haq, B. & Von Rad, U. (1992). *Exmouth Plateau Revisited: Scientific Drilling and Geological Framework*. In: *Proceedings of the Ocean Drilling Program, Scientific Results* (Ed. by U. Von Rad, B. U. Haq, R. B. Kidd & S. B. O'Connell), **122**, 3-20. Ocean Drilling Program, College Station, TX.

Exon, N.F. & Willcox, J.B. (1980) *The Exmouth Plateau: Stratigraphy, Structure, and Petroleum Potential*. Australian Government Publishing Service, Canberra.

Falvey, D. & Veevers, J. (1974) Physiography of the Exmouth and Scott Plateaus, Western Australia, and Adjacent Northeast Wharton Basin. *Marine Geology*, **17,** 21-59

Faugères, J.-C. & Stow, D.A. (1993) Bottom-Current-Controlled Sedimentation: A Synthesis of the Contourite Problem. *Sedimentary Geology*, **82,** 287-297

Faugères, J.-C., Stow, D.A., Imbert, P. & Viana, A. (1999) Seismic Features Diagnostic of Contourite Drifts. *Marine Geology*, **162,** 1-38

Faugères, J.-C. & Stow, D. (2008) Contourite Drifts: Nature, Evolution and Controls. *Developments in sedimentology*, **60,** 257-288

Flood, R.D. (1988) A Lee Wave Model for Deep-Sea Mudwave Activity. *Deep Sea Research Part A. Oceanographic Research Papers*, **35,** 973-983

Gamboa, D., Alves, T., Cartwright, J. & Terrinha, P. (2010) MTD Distribution on a 'Passive' Continental Margin: The Espírito Santo Basin (Se Brazil) During the Palaeogene. *Marine and Petroleum Geology*, **27,** 1311-1324

García, M., Ercilla, G. & Alonso, B. (2009) Morphology and Sedimentary Systems in the Central Bransfield Basin, Antarctic Peninsula: Sedimentary Dynamics from Shelf to Basin. *Basin Research*, **21,** 295-314

Golovchenko, X., Borella, P.E. & O'Connell, S.B. (1992) Sedimentary Cycles on the Exmouth Plateau. In: *Proceedings of the Ocean Drilling Program, Scientific Results* (Ed. by U. Von Rad, B. U. Haq, R. B. Kidd & S. B. O'Connell), **122**, 279-291. Ocean Drilling Program, College Station, TX.

Gong, C., Peakall, J., Wang, Y., Wells, M.G. & Xu, J. (2017) Flow Processes and Sedimentation in Contourite Channels on the Northwestern South China Sea Margin: A Joint 3D Seismic and Oceanographic Perspective. *Marine Geology*, **393,** 176-193

Gradstein, F.M., Ogg, J.G., Schmitz, M. & Ogg, G. (2012) *The Geologic Time Scale 2012*. Elsevier.

Gruetzner, J. & Uenzelmann-Neben, G. (2016) Contourite Drifts as Indicators of Cenozoic Bottom Water Intensity in the Eastern Agulhas Ridge Area, South Atlantic. *Marine Geology*, **378,** 350-360

Hampton, M.A., Lee, H.J. & Locat, J. (1996) Submarine Landslides. *Reviews of Geophysics*, **34,** 33-59

Haq, B.U., Hardenbol, J. & Vail, P.R. (1987) Chronology of Fluctuating Sea Levels since the Triassic. *Science*, **235,** 1156-1167

HAQ, B.U., BOYD, R.L., EXON, N.F. & VON RAD, U. (1992) Evolution of the Central Exmouth Plateau: A Post-Drilling Perspective. In: *Proceedings of the Ocean Drilling Program, Scientific Results* (Ed. by U. Von Rad, B. U. Haq, R. B. Kidd & S. B. O'Connell), **122**, 801-816. Ocean Drilling Program, College Station, TX.

HEINIO, P. & DAVIES, R. (2006) Degradation of Compressional Fold Belts: Deep-Water Niger Delta. *AAPG Bulletin*, **90,** 753-770

HENGESH, J.V., DIRSTEIN, J.K. & STANLEY, A.J. (2013) Landslide Geomorphology Along the Exmouth Plateau Continental Margin, North West Shelf, Australia. *Australian Geomechanics J*, **48,** 71-92

HERNÁNDEZ-MOLINA, F., LARTER, R., REBESCO, M. & MALDONADO, A. (2006a) Miocene Reversal of Bottom Water Flow Along the Pacific Margin of the Antarctic Peninsula: Stratigraphic Evidence from a Contourite Sedimentary Tail. *Marine Geology*, **228,** 93-116

HERNÁNDEZ-MOLINA, F., LLAVE, E. & STOW, D. (2008) Continental Slope Contourites. *Developments in Sedimentology*, **60,** 379-408

HERNÁNDEZ-MOLINA, F.J., LLAVE, E., STOW, D., GARCÍA, M., SOMOZA, L., VÁZQUEZ, J.T., LOBO, F., MAESTRO, A., DEL RÍO, V.D. & LEÓN, R. (2006b) The Contourite Depositional System of the Gulf of Cadiz: A Sedimentary Model Related to the Bottom Current Activity of the Mediterranean Outflow Water and Its Interaction with the Continental Margin. *Deep Sea Research Part II: Topical Studies in Oceanography*, **53,** 1420-1463

HERNÁNDEZ-MOLINA, F.J., SOTO, M., PIOLA, A.R., TOMASINI, J., PREU, B., THOMPSON, P., BADALINI, G., CREASER, A., VIOLANTE, R.A. & MORALES, E. (2016) A Contourite Depositional System Along the Uruguayan Continental Margin: Sedimentary, Oceanographic and Paleoceanographic Implications. *Marine Geology*, **378,** 333-349

HOFSTRA, M., PEAKALL, J., HODGSON, D. & STEVENSON, C. (2018) Architecture and Morphodynamics of Subcritical Sediment Waves in an Ancient Channel–Lobe Transition Zone. *Sedimentology***,** doi:10.1111/sed.12468

Hull, J.N.F. & Griffiths, C.M. (2002). *Sequence Stratigraphic Evolution of the Albian to Recent Section of the Dampier Sub-Basin, Northwest Shelf, Australia*. The Sedimentary Basins of Western Australia 3: Proceedings of the Petroleum Exploration Society of Australia Symposium, Perth.

Huneke, H. & Mulder, T. (2010) *Deep-Sea Sediments*. Elsevier.

Hyndman, R. & Spence, G. (1992) A Seismic Study of Methane Hydrate Marine Bottom Simulating Reflectors. *Journal of Geophysical Research: Solid Earth*, **97,** 6683-6698

Imbert, P. & Ho, S. (2012) Seismic-Scale Funnel-Shaped Collapse Features from the Paleocene–Eocene of the North West Shelf of Australia. *Marine Geology*, **332,** 198-221

James, N.P., Bone, Y., Kyser, T.K., Dix, G.R. & Collins, L.B. (2004) The Importance of Changing Oceanography in Controlling Late Quaternary Carbonate Sedimentation on a High-Energy, Tropical, Oceanic Ramp: North-Western Australia. *Sedimentology*, **51,** 1179-1205

Johnson, D.A. & Damuth, J.E. (1979) Deep Thermohaline Flow and Current-Controlled Sedimentation in the Amirante Passage: Western Indian Ocean. *Marine Geology*, **33,** 1-44

Kähler, G. & Stow, D.A. (1998) Turbidites and Contourites of the Palaeogene Lefkara Formation, Southern Cyprus. *Sedimentary Geology*, **115,** 215-231

Karas, C., Nürnberg, D., Tiedemann, R. & Garbe-Schönberg, D. (2011) Pliocene Indonesian Throughflow and Leeuwin Current Dynamics: Implications for Indian Ocean Polar Heat Flux. *Paleoceanography*, **26,** PA2217

Karner, G.D. & Driscoll, N.W. (1999) Style, Timing and Distribution of Tectonic Deformation across the Exmouth Plateau, Northwest Australia, Determined from Stratal Architecture and Quantitative Basin Modelling. *Geological Society, London, Special Publications*, **164,** 271-311

Keep, M., Powell, C. & Baillie, P. (1998) Neogene Deformation of the North West Shelf, Australia. *The sedimentary basins of Western Australia*, **2,** 81-91

Keep, M., Harrowfield, M. & Crowe, W. (2007) The Neogene Tectonic History of the North West Shelf, Australia. *Exploration Geophysics*, **38,** 151-174

Kelman, A.P., Nicoll, R.S., Kennard, J.M., Mory, A.J., Mantle, D.J., Poidevin, S.L., Bernardel, G., Rollet, N. & Edwards, D. (2013) Northern Carnarvon Basin Biozonation and Stratigraphy, Chart 36, Geoscience Australia

Knutz, P. (2008) Palaeoceanographic Significance of Contourite Drifts. *Developments in Sedimentology*, **60,** 511-535

Llave, E., Jané, G., Maestro, A., López-Martínez, J., Hernández-Molina, F.J. & Mink, S. (2018) Geomorphological and Sedimentary Processes of the Glacially Influenced Northwestern Iberian Continental Margin and Abyssal Plains. *Geomorphology*, **312,** 60-85

Locat, J. & Lee, H.J. (2002) Submarine Landslides: Advances and Challenges. *Canadian Geotechnical Journal*, **39,** 193-212

Lonergan, L., Jamin, N.H., Jackson, C.A.-L. & Johnson, H.D. (2013) U-Shaped Slope Gully Systems and Sediment Waves on the Passive Margin of Gabon (West Africa). *Marine Geology*, **337,** 80-97

Longley, I.M., Buessenschuett, C., Clydsdale, L., Cubitt, C.J., Davis, R.C., Johnson, M.K., Marshall, N.M., Murray, A.P., Somerville, R. & Spry, T.B. (2002) The North West Shelf of Australia - a Woodside Perspective. *The Sedimentary Basins of Western Australia 3: Petroleum Exploration Society of Australia Symposium*. M. Keep & S. J. Moss. Perth**,** 28-88

Marchès, E., Mulder, T., Gonthier, E., Cremer, M., Hanquiez, V., Garlan, T. & Lecroart, P. (2010) Perched Lobe Formation in the Gulf of Cadiz: Interactions between Gravity Processes and Contour Currents (Algarve Margin, Southern Portugal). *Sedimentary Geology*, **229,** 81-94

Martorelli, E., Bosman, A., Casalbore, D. & Falcini, F. (2016) Interaction of Down-Slope and Along-Slope Processes Off Capo Vaticano (Southern Tyrrhenian Sea, Italy), with Particular Reference to Contourite-Related Landslides. *Marine Geology*, **378,** 43-55

Martos, Y.M., Maldonado, A., Lobo, F.J., Hernández-Molina, F.J. & Pérez, L.F. (2013) Tectonics and Palaeoceanographic Evolution Recorded by Contourite Features in Southern Drake Passage (Antarctica). *Marine Geology*, **343,** 76-91

Masson, D., Wynn, R. & Talling, P. (2010) Large Landslides on Passive Continental Margins: Processes, Hypotheses and Outstanding Questions. In: *Submarine Mass Movements and Their Consequences* (Ed. by D. C. Mosher, C. Shipp, L. Moscardelli, J. D. Chaytor, C. D. P. Baxter, H. J. Lee & R. Urgeles), 153-165. Springer, Dordrecht.

Michels, K.H., Rogenhagen, J. & Kuhn, G. (2001) Recognition of Contour-Current Influence in Mixed Contourite-Turbidite Sequences of the Western Weddell Sea, Antarctica. *Marine Geophysical Researches*, **22,** 465-485

Miller, K.G., Wright, J.D. & Fairbanks, R.G. (1991) Unlocking the Ice House: Oligocene-Miocene Oxygen Isotopes, Eustasy, and Margin Erosion. *Journal of Geophysical Research: Solid Earth*, **96,** 6829-6848

Mulder, T., Lecroart, T., Voisset, M., Schönfeld, J., Le Drezen, E., Gonthier, E., Hanquiez, V., Zahn, R., Faugères, J.C. & Hernandez-Molina, F. (2002) Past Deep-Ocean Circulation and the Paleoclimate Record-Gulf of Cadiz. *EOS, Transactions American Geophysical Union*, **83,** 481-488

Mulder, T., Lecroart, P., Hanquiez, V., Marches, E., Gonthier, E., Guedes, J.-C., Thiébot, E., Jaaidi, B., Kenyon, N. & Voisset, M. (2006) The Western Part of the Gulf of Cadiz: Contour Currents and Turbidity Currents Interactions. *Geo-Marine Letters*, **26,** 31-41

Müller, R., Dyksterhuis, S. & Rey, P. (2012) Australian Paleo-Stress Fields and Tectonic Reactivation over the Past 100 Ma. *Australian Journal of Earth Sciences*, **59,** 13-28

Murgese, D.S. & De Deckker, P. (2007) The Late Quaternary Evolution of Water Masses in the Eastern Indian Ocean between Australia and Indonesia, Based on Benthic Foraminifera Faunal and Carbon Isotopes Analyses. *Palaeogeography, Palaeoclimatology, Palaeoecology*, **247,** 382-401

Ortiz-Karpf, A., Hodgson, D.M., Jackson, C.A.L. & McCaffrey, W.D. (2016) Mass-Transport Complexes as Markers of Deep-Water Fold-and-Thrust Belt Evolution: Insights from the Southern Magdalena Fan, Offshore Colombia. *Basin Research*, **30,** 65-88

Osborne, M.J. & Swarbrick, R.E. (1997) Mechanisms for Generating Overpressure in Sedimentary Basins: A Reevaluation. *AAPG bulletin*, **81,** 1023-1041

Pearce, A. (1991) Eastern Boundary Currents of the Southern Hemisphere. *Journal of the Royal Society of Western Australia*, **74,** 35-45

Pérez, L.F., Maldonado, A., Bohoyo, F., Hernández-Molina, F.J., Vázquez, J.T., Lobo, F.J. & Martos, Y.M. (2014) Depositional Processes and Growth Patterns of Isolated Oceanic Basins: The Protector and Pirie Basins of the Southern Scotia Sea (Antarctica). *Marine Geology*, **357,** 163-181

Pérez, L.F., Bohoyo, F., Hernández-Molina, F.J., Casas, D., Galindo-Zaldívar, J., Ruano, P. & Maldonado, A. (2016) Tectonic Activity Evolution of the Scotia-Antarctic Plate Boundary from Mass Transport Deposit Analysis. *Journal of Geophysical Research: Solid Earth*, **121,** 2216-2234

Pérez, L.F., Maldonado, A., Hernández-Molina, F.J., Lodolo, E., Bohoyo, F. & Galindo-Zaldívar, J. (2017) Tectonic and Oceanographic Control of Sedimentary Patterns in a Small Oceanic Basin: Dove Basin (Scotia Sea, Antarctica). *Basin Research*, **29,** 255-276

Pickering, K.T., Hiscott, R.N. & Hein, F.J. (1989) *Deep-Marine Environments: Clastic Sedimentation and Tectonics*. Allen & Unwin Australia.

Powell, C.M., Roots, S. & Veevers, J. (1988) Pre-Breakup Continental Extension in East Gondwanaland and the Early Opening of the Eastern Indian Ocean. *Tectonophysics*, **155,** 261-283

Rebesco, M., Hernández-Molina, F.J., Van Rooij, D. & Wåhlin, A. (2014) Contourites and Associated Sediments Controlled by Deep-Water Circulation Processes: State-of-the-Art and Future Considerations. *Marine Geology*, **352,** 111-154

Reed, D.L., Meyer, A.W., Silver, E.A. & Prasetyo, H. (1987) Contourite Sedimentation in an Intraoceanic Forearc System: Eastern Sunda Arc, Indonesia. *Marine Geology*, **76,** 223-241

Richardson, S.E.J., Davies, R.J., Allen, M.B. & Grant, S.F. (2011) Structure and Evolution of Mass Transport Deposits in the South Caspian Basin, Azerbaijan. *Basin Research*, **23,** 702-719

ROMERO-OTERO, G.A., SLATT, R.M. & PIRMEZ, C. (2010) Detached and Shelf-Attached Mass Transport Complexes on the Magdalena Deepwater Fan. In: *Submarine Mass Movements and Their Consequences* (Ed. by D. C. Mosher, C. Shipp, L. Moscardelli, J. D. Chaytor, C. D. P. Baxter, H. J. Lee & R. Urgeles), 593-606. Springer, Dordrecth.

ROMINE, K., DURRANT, J., CATHRO, D. & BERNARDEL, G. (1997) Petroleum Play Element Prediction for the Cretaceous–Tertiary Basin Phase, Northern Carnarvon Basin. *APPEA*, **37,** 315-339

SALLES, T., MARCHÈS, E., DYT, C., GRIFFITHS, C., HANQUIEZ, V. & MULDER, T. (2010) Simulation of the Interactions between Gravity Processes and Contour Currents on the Algarve Margin (South Portugal) Using the Stratigraphic Forward Model Sedsim. *Sedimentary Geology*, **229,** 95-109

SCARSELLI, N., MCCLAY, K. & ELDERS, C. (2013). *Submarine Slide and Slump Complexes, Exmouth Plateau, NW Shelf of Australia*. The Sedimentary Basins of Western Australia IV: Proceedings of the Petroleum Exploration Society of Australia Symposium, Perth.

SCARSELLI, N., MCCLAY, K. & ELDERS, C. (2016) Seismic Geomorphology of Cretaceous Megaslides Offshore Namibia (Orange Basin): Insights into Segmentation and Degradation of Gravity-Driven Linked Systems. *Marine and Petroleum Geology*, **75,** 151-180

SHANMUGAM, G., SPALDING, T. & ROFHEART, D. (1993) Process Sedimentology and Reservoir Quality of Deep-Marine Bottom-Current Reworked Sands (Sandy Contourites): An Example from the Gulf of Mexico. *AAPG Bulletin*, **77,** 1241-1259

SINHA, D.K., SINGH, A.K. & TIWARI, M. (2006) Palaeoceanographic and Palaeoclimatic History of ODP Site 763a (Exmouth Plateau), Southeast Indian Ocean: 2.2 Ma Record of Planktic Foraminifera. *Current Science***,** 1363-1369

SMITH, R.L., HUYER, A., GODFREY, J.S. & CHURCH, J.A. (1991) The Leeuwin Current Off Western Australia, 1986–1987. *Journal of Physical Oceanography*, **21,** 323-345

SOARES, D.M., ALVES, T.M. & TERRINHA, P. (2014) Contourite Drifts on Early Passive Margins as an Indicator of Established Lithospheric Breakup. *Earth and Planetary Science Letters*, **401,** 116-131

Spooner, M.I., De Deckker, P., Barrows, T.T. & Fifield, L.K. (2011) The Behaviour of the Leeuwin Current Offshore NW Australia During the Last Five Glacial–Interglacial Cycles. *Global and Planetary Change*, **75,** 119-132

Stow, D.A., Hernández-Molina, F.J., Llave, E., Sayago-Gil, M., Díaz del Río, V. & Branson, A. (2009) Bedform-Velocity Matrix: The Estimation of Bottom Current Velocity from Bedform Observations. *Geology*, **37,** 327-330

Symons, W.O., Sumner, E.J., Talling, P.J., Cartigny, M.J. & Clare, M.A. (2016) Large-Scale Sediment Waves and Scours on the Modern Seafloor and Their Implications for the Prevalence of Supercritical Flows. *Marine Geology*, **371,** 130-148

Tchernia, P. (1980) *Descriptive Regional Oceanography*. Pergamon.

Thöle, H., Kuhlmann, G., Lutz, R. & Gaedicke, C. (2016) Late Cenozoic Submarine Slope Failures in the Southern North Sea–Evolution and Controlling Factors. *Marine and Petroleum Geology*, **75,** 272-290

Tindale, K., Newell, N., Keall, J. & Smith, N. (1998) Structural Evolution and Charge History of the Exmouth Sub-Basin, Northern Carnarvon Basin, Western Australia. In: *The Sedimentary Basins of Western Australia 2: Proceedings of the Petroleum Exploration Society of Australia* (Ed. by P. G. Purcell & R. R. Purcell), 473-490, Perth.

Uenzelmann-Neben, G. (2002) Contourites on the Agulhas Plateau, Sw Indian Ocean: Indications for the Evolution of Currents since Palaeogene Times. *Geological Society, London, Memoirs*, **22,** 271-288

Uenzelmann-Neben, G. (2006) Depositional Patterns at Drift 7, Antarctic Peninsula: Along-Slope Versus Down-Slope Sediment Transport as Indicators for Oceanic Currents and Climatic Conditions. *Marine geology*, **233,** 49-62

Uenzelmann-Neben, G. & Gohl, K. (2012) Amundsen Sea Sediment Drifts: Archives of Modifications in Oceanographic and Climatic Conditions. *Marine Geology*, **299,** 51-62

Vandorpe, T., Van Rooij, D. & De Haas, H. (2014) Stratigraphy and Paleoceanography of a Topography-Controlled Contourite Drift in the Pen Duick Area, Southern Gulf of Cádiz. *Marine Geology*, **349,** 136-151

Veevers, J., Powell, C.M. & Roots, S. (1991) Review of Seafloor Spreading around Australia. I. Synthesis of the Patterns of Spreading. *Australian Journal of Earth Sciences*, **38,** 373-389

Viana, A., Faugères, J.-C. & Stow, D. (1998) Bottom-Current-Controlled Sand Deposits—a Review of Modern Shallow-to Deep-Water Environments. *Sedimentary Geology*, **115,** 53-80

Vinnels, J.S., Butler, R.W., McCaffrey, W.D. & Paton, D.A. (2010) Depositional Processes across the Sinú Accretionary Prism, Offshore Colombia. *Marine and Petroleum Geology*, **27,** 794-809

Völker, D., Geersen, J., Behrmann, J.H. & Weinrebe, W.R. (2012) Submarine Mass Wasting Off Southern Central Chile: Distribution and Possible Mechanisms of Slope Failure at an Active Continental Margin. In: *Submarine Mass Movements and Their Consequences* (Ed. by Y. Yamada, K. Kawamura, K. Ikehara, Y. Ogawa, R. Urgeles, D. C. Mosher, J. D. Chaytor & M. Strasser), 379-389. Springer, Dordrecht.

Wells, P.E. & Wells, G.M. (1994) Large-Scale Reorganization of Ocean Currents Offshore Western Australia During the Late Quaternary. *Marine Micropaleontology*, **24,** 157-186

Wynn, R.B. & Stow, D.A. (2002) Classification and Characterisation of Deep-Water Sediment Waves. *Marine Geology*, **192,** 7-22

10. Figure Captions

Figure 1. The location of the study area, the Exmouth Plateau (EP), to the south of the plate boundary (bold black line), where the Australian Plate subducts beneath the Eurasian Plate. Ocean current pathways are modified from Collins *et al.* (2014) and Spooner *et al.* (2011). Abbreviations are: LC: Leeuwin Current; SEC: South Equatorial Current; WAC: West Australian Current; AR: Argo Abyssal Plain; GA: Gascoyne Abyssal Plain; CU: Cuvier Abyssal Plain; EP: Exmouth Plateau. Shaded relief GEBCO_2014 bathymetry map downloaded from https://www.ngdc.noaa.gov/maps/autogrid/ (accessed on 20 February 2018, 2.41 pm GMT).

Figure 2. Tectonostratigraphic framework of the Exmouth Plateau (modified from Kelman *et al.* (2013), the palaeo-water depth is inferred from Hull and Griffiths (2002), the sea-level curve is from Haq *et al.* (1987), geological time-scale from Gradstein *et al.* (2012), and tectonic events are compiled from references discussed in the text. Four regional horizons (Horizon A, B, C, and D) are mapped across the study area, which define three seismic units: SU-1, SU-2, and SU-3.

Figure 3. Location map of the study area (blue polygon) and the distribution of seismic reflection and well data. The blue polygon defines the total area; the grey lines represent 2D seismic data and the black polygon defines the 3D seismic volume (Duyfken). Wells used in this study are coloured in green. The regional 2D seismic line (in orange) is shown in Figure 4. Abbreviations for the North Carnarvon Sub-basins are as follows: BA: Barrow Sub-basin; BE: Beagle Sub-basin; DA: Dampier Sub-basin; EP: Exmouth Plateau; EX: Exmouth Sub-basin; RP: Rankin Platform; CRFZ: Cape Range Fracture Zone. Sub-basins outline and topography grid are from Geoscience Australia.

Figure 4. Regional 2D seismic line across the study area (a) uninterpreted, and (b) interpreted. Four regional horizons (Horizon A-D) have been mapped, which define three seismic units: SU-1, SU-2, and SU-3.

Figure 5. A simplified well correlation panel showing gross lithology distribution and stratigraphic relationships, based on core data (ODP 762) and ditch cuttings (other wells). Datum is Top Muderong Shale (Aptian). See Figure 3 for well locations on map and Figure 4 for well locations on regional seismic section.

Figure 6. General seismic facies characteristics observed in each seismic unit.

Figure 7. Representative seismic sections showing the main seismic facies characteristics of each seismic unit. The location of each seismic line is shown in Figure 8a.

Figure 8. (a) Base map showing the location of seismic sections (Fig. 6), wells and the main present-day bathymetric structural features. (b) Depth structure map of Horizon A. (c-e) Isopach maps (left) and seismic facies map (right) of each seismic unit.

Figure 9. (a) Depth structure map of Horizon A within 3D seismic area. (b) RMS amplitude extraction from Horizon A. Note the slightly curved, mainly straight to very low-sinuosity lineations. The sinuous lineations (SW area) are roughly parallel to the trend of SU-1 contourite channel (Fig. 7c), and the dominant, NE-SW oriented, straight lineations (central area). (c) Seismic section across the sinuous lineations in Figure 9b showing SU-1 contourites channel. (d) Seismic section across the straight lineations in Figure 9b showing mounded erosional surface interpreted as erosional remnants.

Figure 10. (a) Seismic section across the transition zone into the VFZ. (b-d) Shaded relief depth structure maps (left) and interpretive sketches (right) of Horizon C-2, C-3, and C-4.

Figure 11. (a) Detailed strike seismic section of multiple occurrences of MTCs (i.e. MTC-1, 2 and 3) in the Kangaroo Syncline. Variance maps showing (b) lateral margin and remnant blocks within the MTC-1 body, (c) grooves on MTC-2 basal shear surface, and (d) primary and secondary flow fabrics (PFFs and SFFs) on MTC-3 top surface (seabed).

Figure 12. Plate configurations around Australia during: (a) 96 Ma Late Cretaceous; (b) 64 Ma early Palaeocene; (c) 35.5 Ma early Oligocene; (d) 10 Ma late Miocene. See text for discussion. Ocean floor colours represent phases of seafloor spreading based on magnetic anomaly, from oldest to youngest: (i) Phase 1: Blue; (ii) Phase 1: Green; and (iii) Phase 3: Orange. Maps are modified from Veevers *et al.* (1991).

843 Fig. 1

844 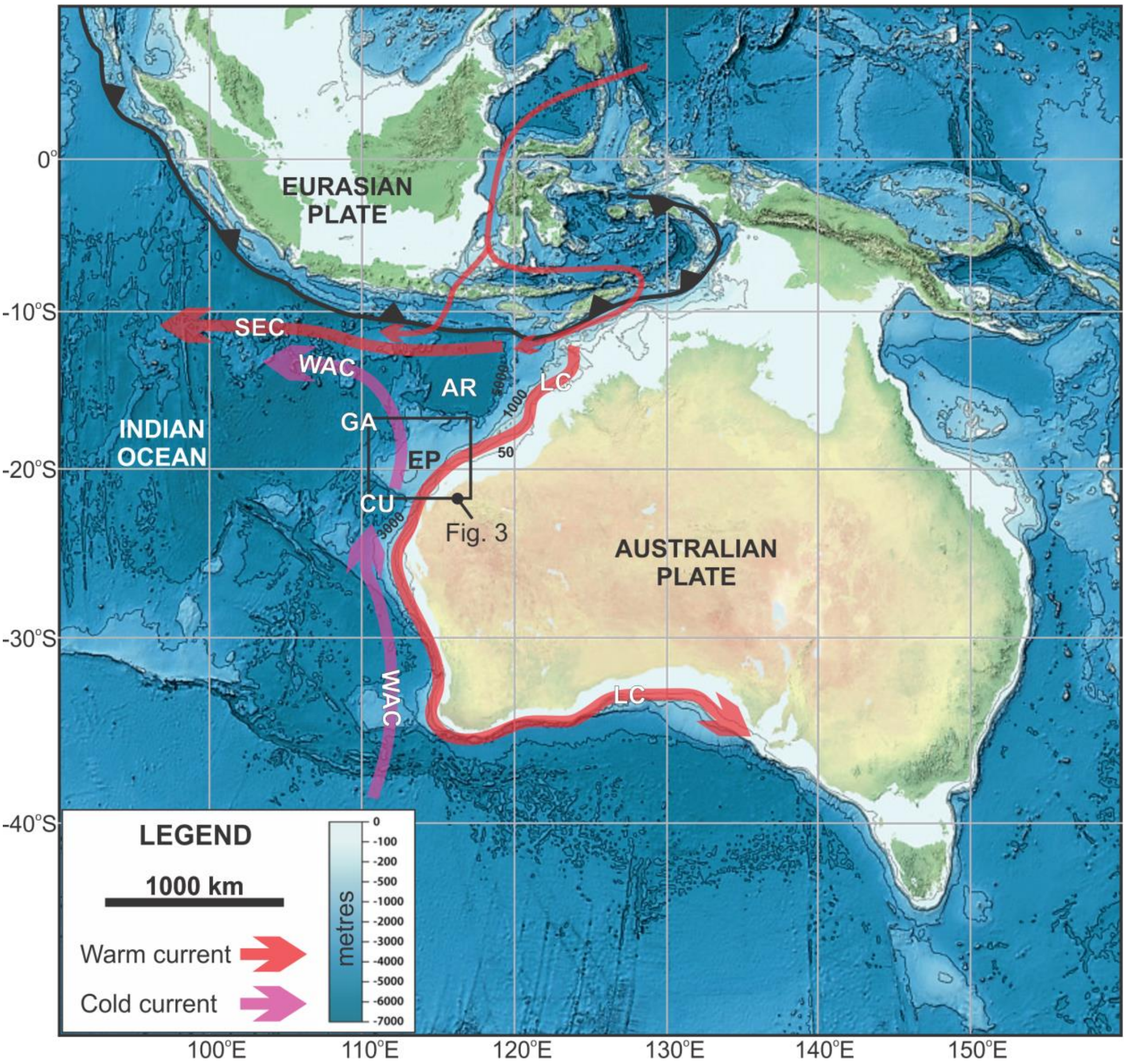
EURASIAN PLATE
AUSTRALIAN PLATE
INDIAN OCEAN
SEC
WAC
AR
GA
EP
CU
LC
Fig. 3
LEGEND
1000 km
Warm current
Cold current
metres
0°
-10°S
-20°S
-30°S
-40°S
100°E
110°E
120°E
130°E
140°E
150°E

Fig. 2

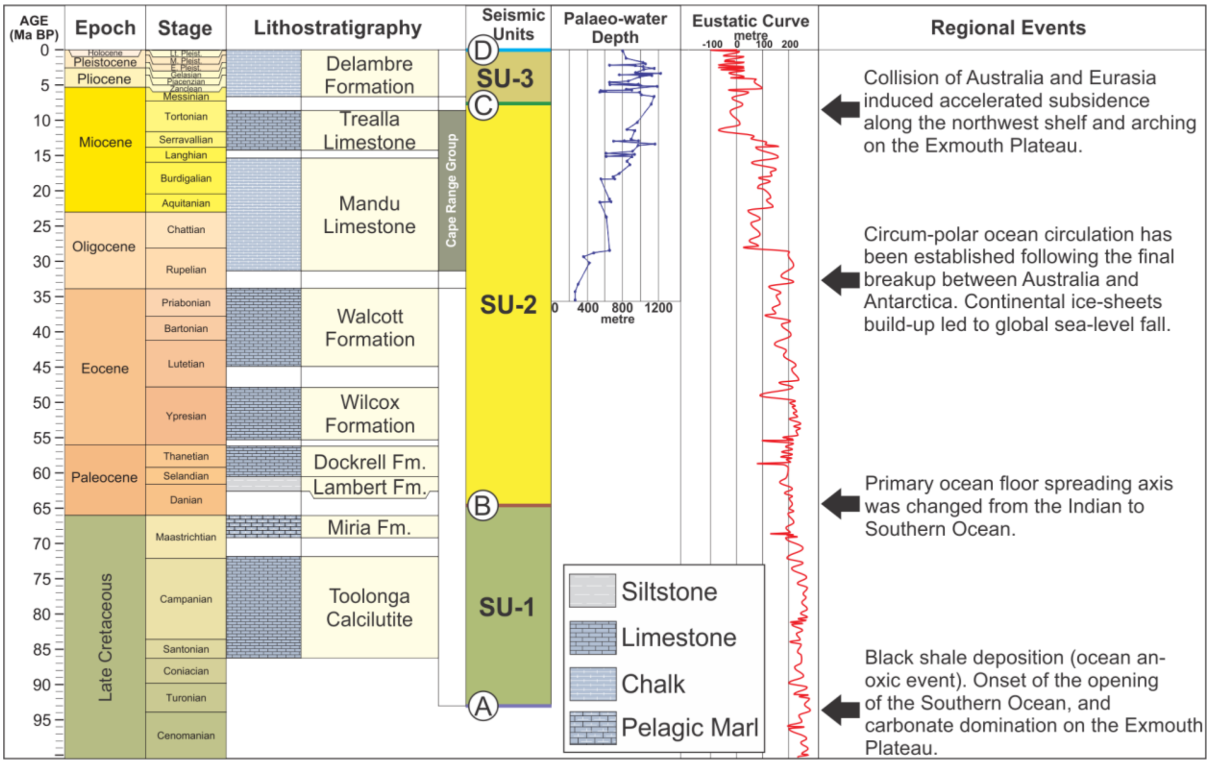
AGE (Ma BP)
Epoch
Stage
Lithostratigraphy
Seismic Units
Palaeo-water Depth
Eustatic Curve
Regional Events
Pleistocene
Pliocene
Miocene
Oligocene
Eocene
Paleocene
Late Cretaceous
Messinian
Tortonian
Serravallian
Langhian
Burdigalian
Aquitanian
Chattian
Rupelian
Priabonian
Bartonian
Lutetian
Ypresian
Thanetian
Selandian
Danian
Maastrichtian
Campanian
Santonian
Coniacian
Turonian
Cenomanian
Delambre Formation
Trealla Limestone
Mandu Limestone
Cape Range Group
Walcott Formation
Wilcox Formation
Dockrell Fm.
Lambert Fm.
Miria Fm.
Toolonga Calcilutite
SU-3
SU-2
SU-1
D
C
B
A
0 400 800 1200
metre
-100 0 100 200
metre
Siltstone
Limestone
Chalk
Pelagic Marl
Collision of Australia and Eurasia induced accelerated subsidence along the northwest shelf and arching on the Exmouth Plateau.
Circum-polar ocean circulation has been established following the final breakup between Australia and Antarctica. Continental ice-sheets build-up led to global sea-level fall.
Primary ocean floor spreading axis was changed from the Indian to Southern Ocean.
Black shale deposition (ocean an-oxic event). Onset of the opening of the Southern Ocean, and carbonate domination on the Exmouth Plateau.

Fig. 3

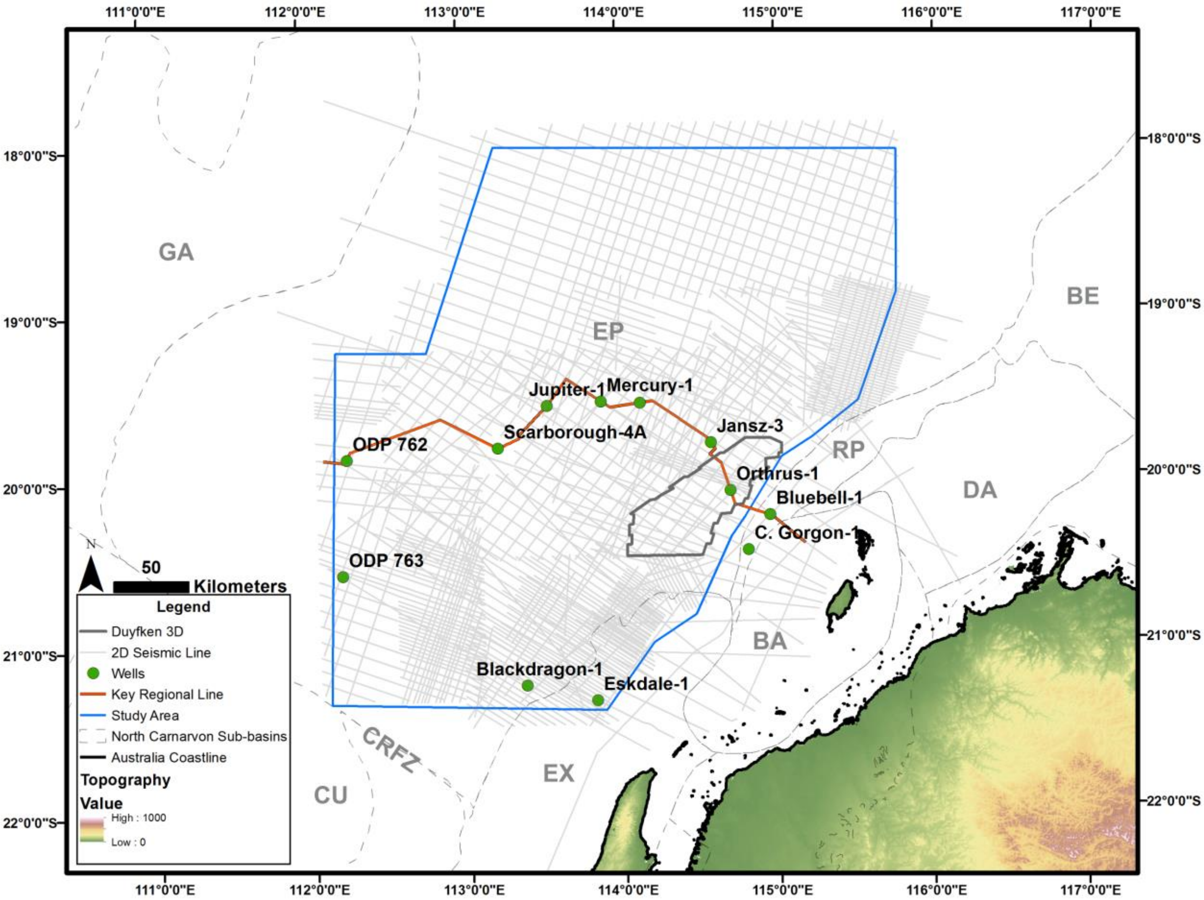
111°0'0"E
112°0'0"E
113°0'0"E
114°0'0"E
115°0'0"E
116°0'0"E
117°0'0"E
18°0'0"S
19°0'0"S
20°0'0"S
21°0'0"S
22°0'0"S
GA
EP
BE
RP
DA
BA
EX
CU
CRFZ
Jupiter-1
Mercury-1
Scarborough-4A
Jansz-3
ODP 762
Orthrus-1
Bluebell-1
C. Gorgon-1
ODP 763
Blackdragon-1
Eskdale-1
N
50
Kilometers
Legend
Duyfken 3D
2D Seismic Line
Wells
Key Regional Line
Study Area
North Carnarvon Sub-basins
Australia Coastline
Topography
Value
High : 1000
Low : 0

Fig. 4

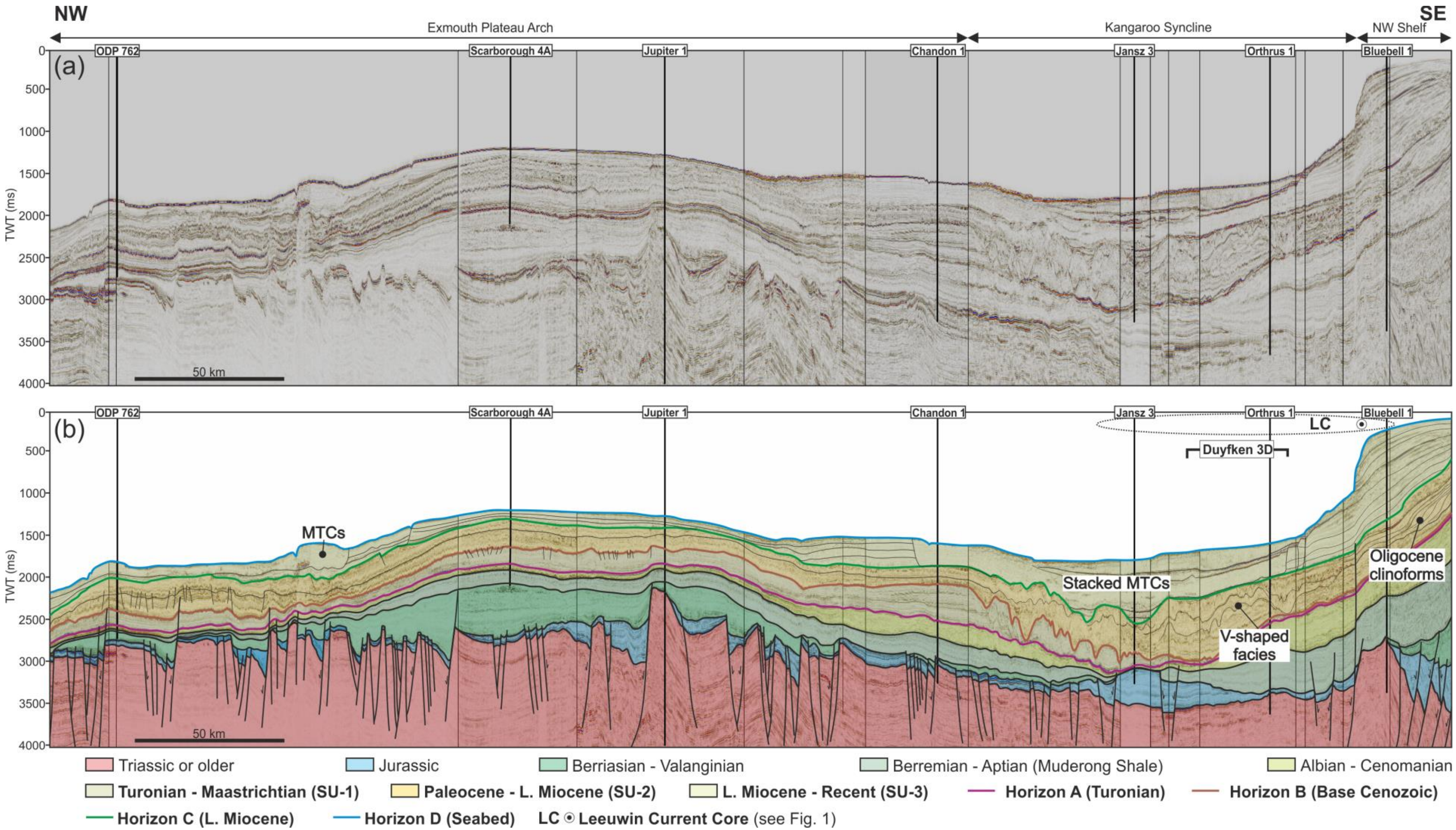
NW
SE
Exmouth Plateau Arch
Kangaroo Syncline
NW Shelf
ODP 762
Scarborough 4A
Jupiter 1
Chandon 1
Jansz 3
Orthrus 1
Bluebell 1
(a)
(b)
TWT (ms)
50 km
MTCs
LC
Duyfken 3D
Stacked MTCs
V-shaped facies
Oligocene clinoforms
Triassic or older
Jurassic
Berriasian - Valanginian
Berremian - Aptian (Muderong Shale)
Albian - Cenomanian
Turonian - Maastrichtian (SU-1)
Paleocene - L. Miocene (SU-2)
L. Miocene - Recent (SU-3)
Horizon A (Turonian)
Horizon B (Base Cenozoic)
Horizon C (L. Miocene)
Horizon D (Seabed)
LC ⊙ Leeuwin Current Core (see Fig. 1)

852 Fig. 5

853 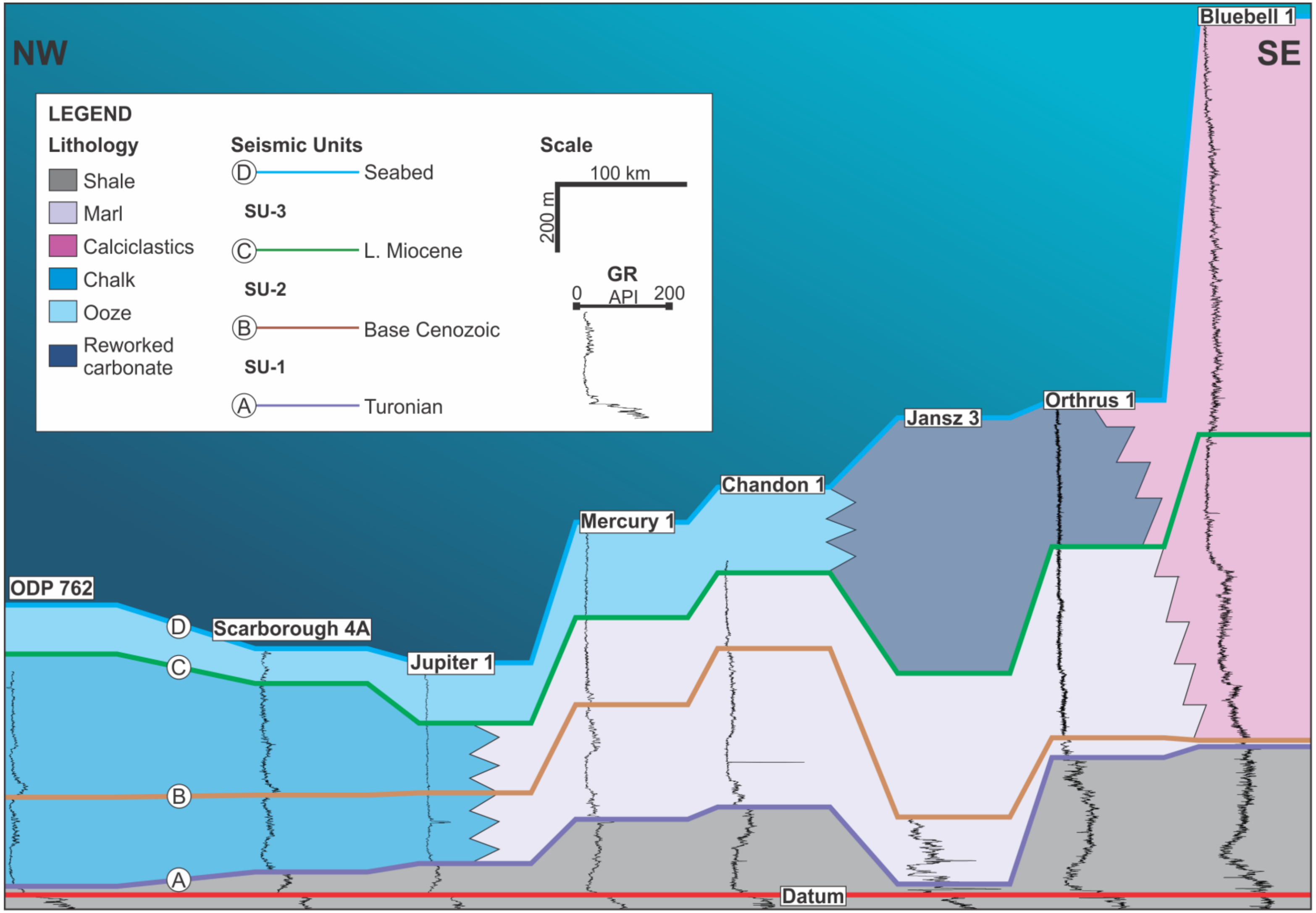
NW
SE
LEGEND
Lithology
Shale
Marl
Calciclastics
Chalk
Ooze
Reworked carbonate
Seismic Units
D Seabed
SU-3
C L. Miocene
SU-2
B Base Cenozoic
SU-1
A Turonian
Scale
100 km
200 m
GR
0 API 200
ODP 762
Scarborough 4A
Jupiter 1
Mercury 1
Chandon 1
Jansz 3
Orthrus 1
Bluebell 1
Datum

Fig. 6

Facies	Description	Example	Interpretation	Occurrences within SU
SF-1	Sub-parallel, continuous, alternating low- to high-amplitude reflections, local offset faults are common in some places.	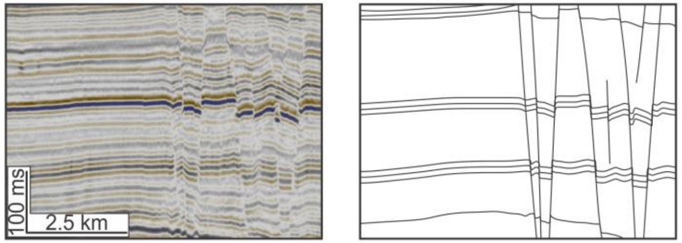	Hemipelagic deposits or sheeted contourite drift (e.g. Faugères et al., 1999).	SU-1 and SU-2: Predominantly in the northern and eastern part of the study area. SU-3: Predominantly around the Exmouth Plateau Arch.
SF-2	Sub-parallel, continuous, alternating low- to high-amplitude with truncated internal reflections. Oriented sub-parallel or oblique with slope in map-view.	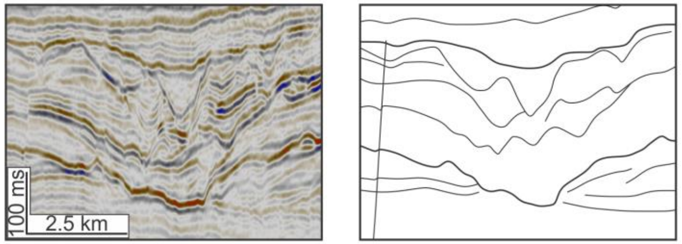	Contourite channel (e.g. Faugères et al., 1999).	SU-1 and SU-2: Predominantly in the eastern part of the study area, along the Kangaroo Syncline.
SF-3	Sub-parallel to wavy, variable low- to high-amplitude, with common v-shaped, internal truncations. Commonly oriented oblique to slope.	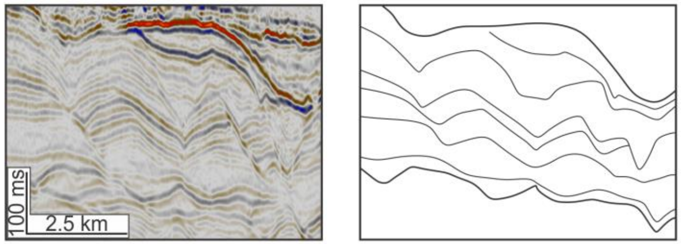	Sediment waves, or erosional remnants of sediment waves (e.g. Faugères et al., 1999).	SU-2: Encountered in the northern part of the Kangaroo Syncline, termed as v-shaped facies zone (VFZ).
SF-4	Discontinuous to chaotic, variable low- to high-amplitude reflections.	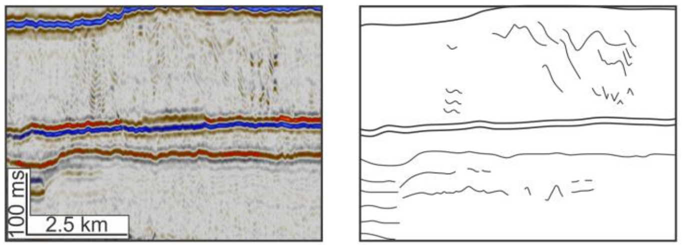	Mass-transport complexes (MTCs) (e.g. Bull et al., 2009)	SU-3: Common in the present-day bathymetric low, such as in the Kangaroo Syncline, and flanks of the Exmouth Plateau Arch.

Fig. 7

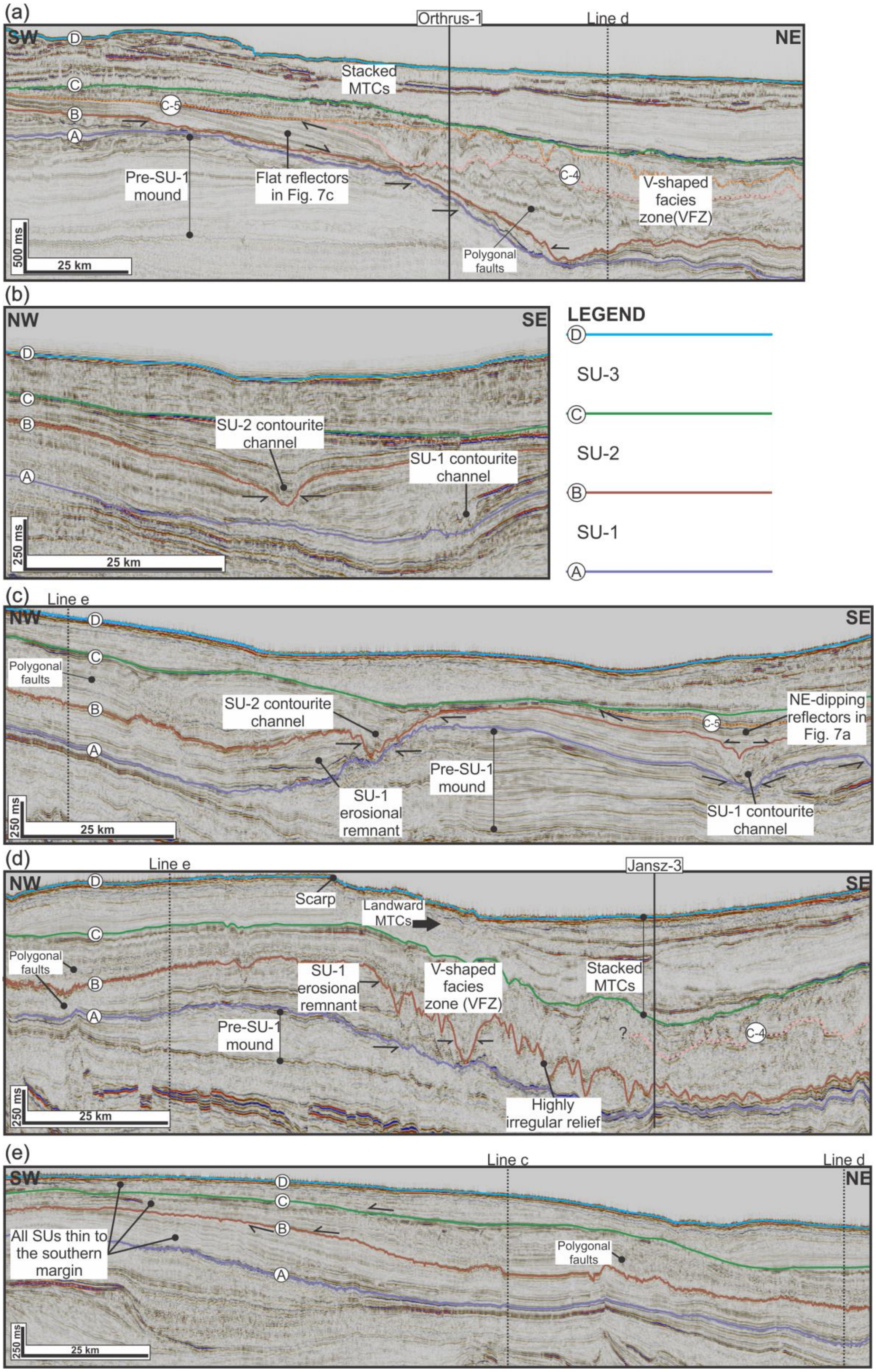
(a)
Orthrus-1
Line d
SW
NE
D
C
B
A
C-5
C-4
Stacked MTCs
Pre-SU-1 mound
Flat reflectors in Fig. 7c
V-shaped facies zone(VFZ)
Polygonal faults
500 ms
25 km
(b)
NW
SE
SU-2 contourite channel
SU-1 contourite channel
250 ms
25 km
LEGEND
SU-3
SU-2
SU-1
(c)
Line e
NW
SE
Polygonal faults
SU-2 contourite channel
NE-dipping reflectors in Fig. 7a
Pre-SU-1 mound
SU-1 erosional remnant
SU-1 contourite channel
250 ms
25 km
(d)
Line e
Jansz-3
NW
SE
Scarp
Landward MTCs
Polygonal faults
SU-1 erosional remnant
V-shaped facies zone (VFZ)
Stacked MTCs
Pre-SU-1 mound
Highly irregular relief
250 ms
25 km
(e)
Line c
Line d
SW
NE
All SUs thin to the southern margin
Polygonal faults
250 ms
25 km

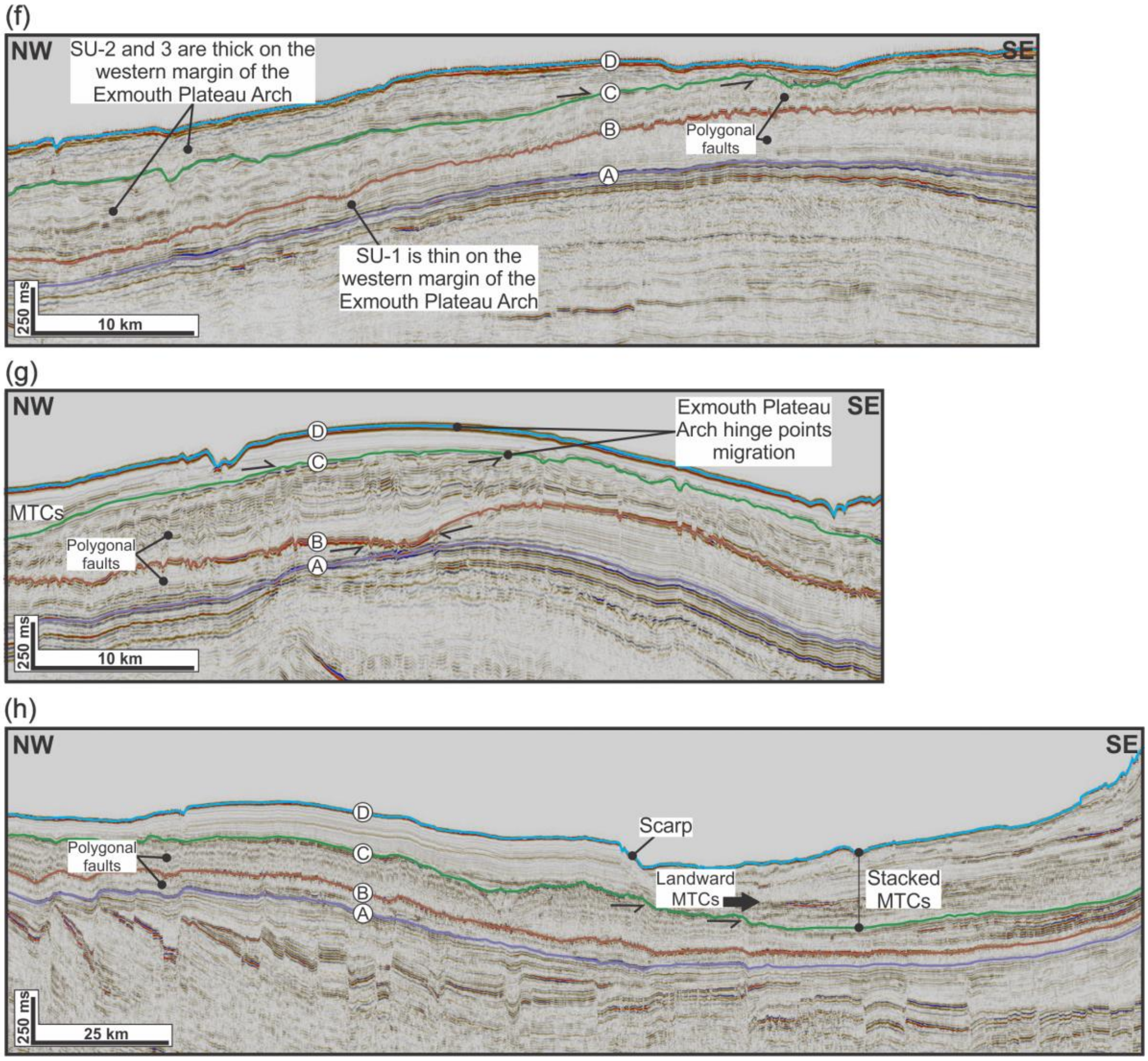
(f)
NW
SE
SU-2 and 3 are thick on the western margin of the Exmouth Plateau Arch
D
C
B
A
Polygonal faults
SU-1 is thin on the western margin of the Exmouth Plateau Arch
250 ms
10 km
(g)
NW
SE
Exmouth Plateau Arch hinge points migration
D
C
B
A
MTCs
Polygonal faults
250 ms
10 km
(h)
NW
SE
D
C
B
A
Scarp
Polygonal faults
Landward MTCs
Stacked MTCs
250 ms
25 km

858

859 Fig. 8

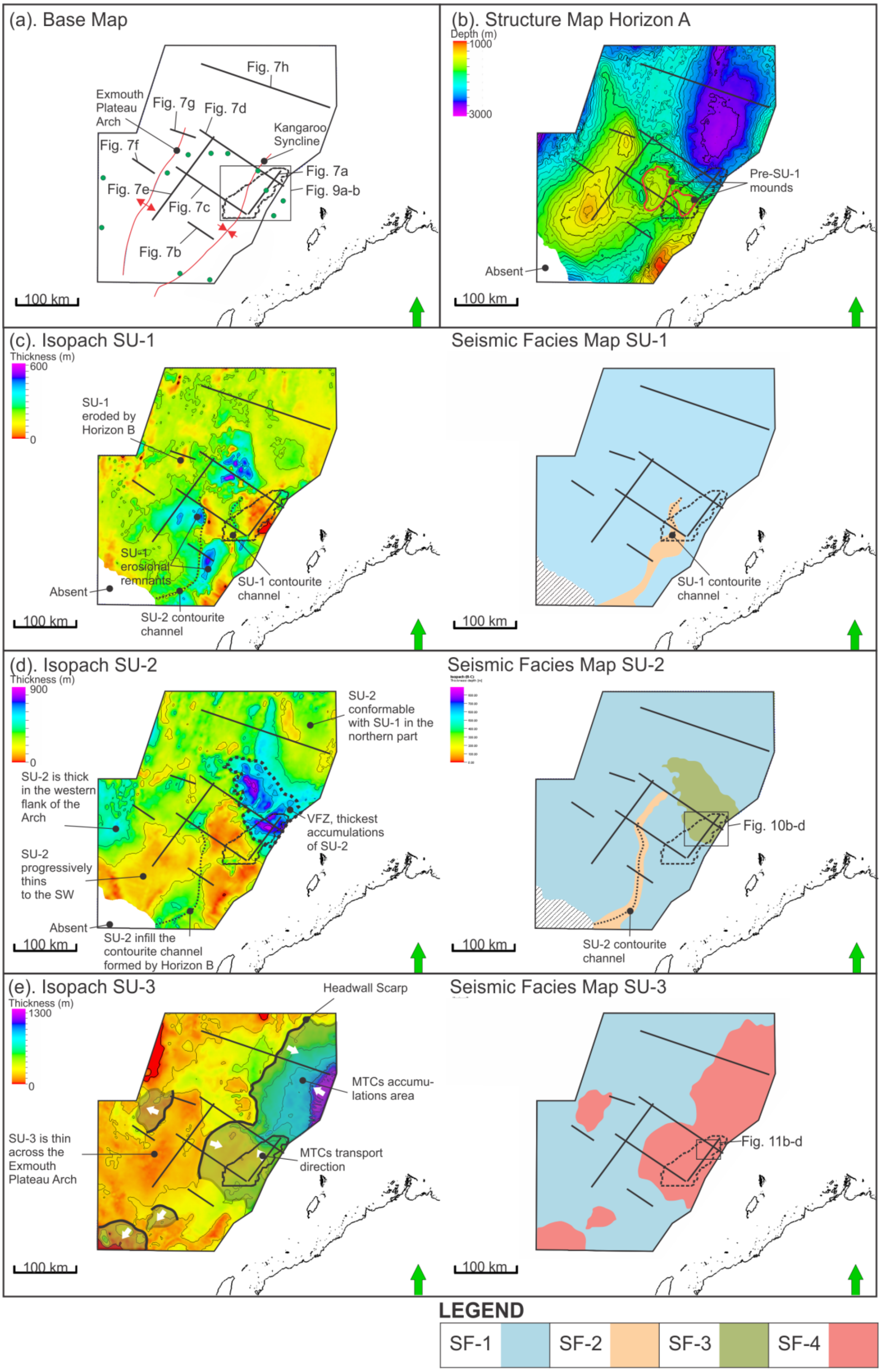
(a). Base Map
Fig. 7h
Exmouth Plateau Arch
Fig. 7g
Fig. 7d
Kangaroo Syncline
Fig. 7f
Fig. 7a
Fig. 9a-b
Fig. 7e
Fig. 7c
Fig. 7b
100 km
(b). Structure Map Horizon A
Depth (m)
1000
3000
Pre-SU-1 mounds
Absent
100 km
(c). Isopach SU-1
Thickness (m)
600
0
SU-1 eroded by Horizon B
SU-1 erosional remnants
Absent
SU-1 contourite channel
SU-2 contourite channel
100 km
Seismic Facies Map SU-1
SU-1 contourite channel
100 km
(d). Isopach SU-2
Thickness (m)
900
0
SU-2 conformable with SU-1 in the northern part
SU-2 is thick in the western flank of the Arch
VFZ, thickest accumulations of SU-2
SU-2 progressively thins to the SW
Absent
SU-2 infill the contourite channel formed by Horizon B
100 km
Seismic Facies Map SU-2
Fig. 10b-d
SU-2 contourite channel
100 km
(e). Isopach SU-3
Thickness (m)
1300
0
Headwall Scarp
MTCs accumu-lations area
SU-3 is thin across the Exmouth Plateau Arch
MTCs transport direction
100 km
Seismic Facies Map SU-3
Fig. 11b-d
100 km
LEGEND
SF-1
SF-2
SF-3
SF-4

860

861 Fig. 9

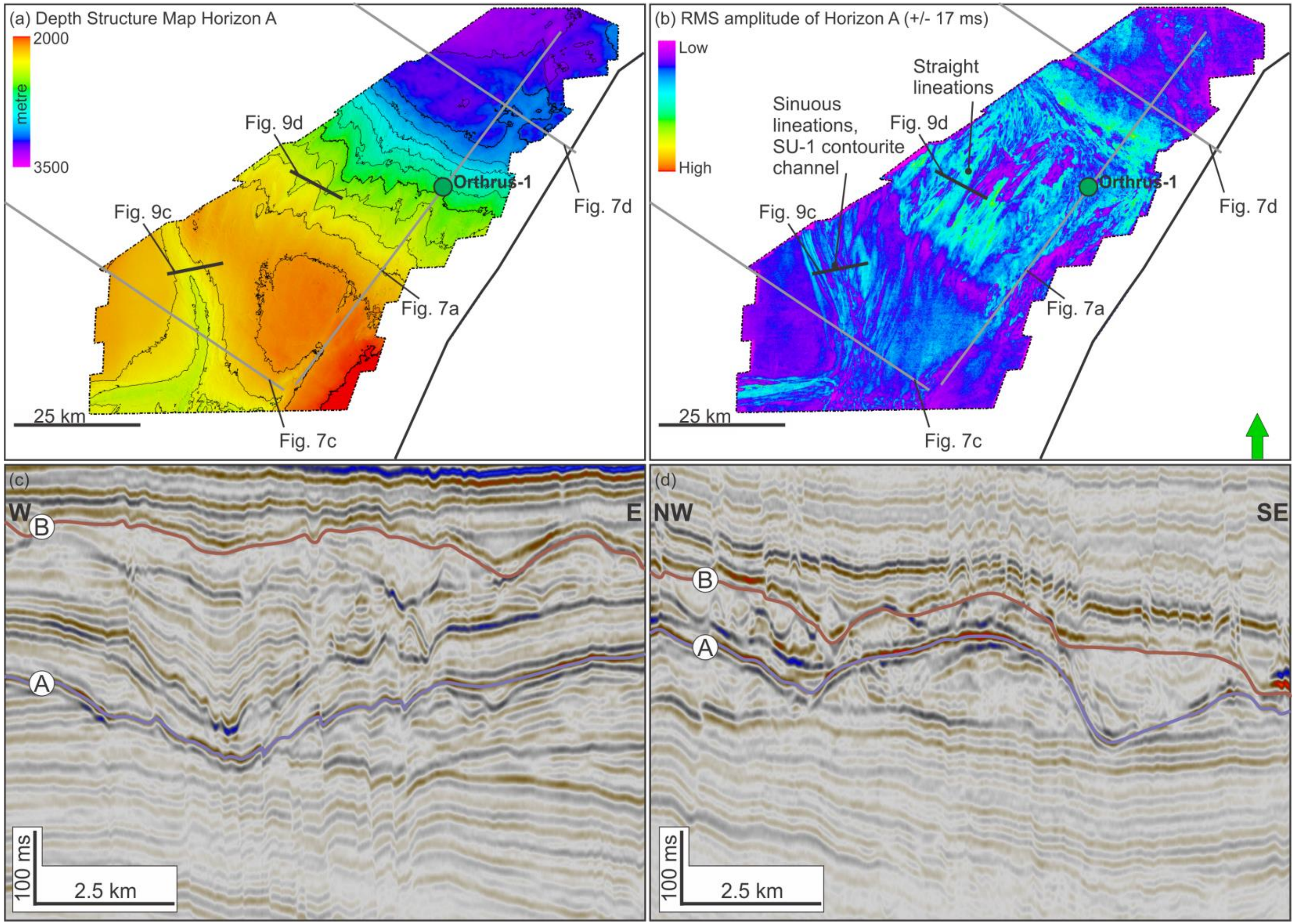

(a) Depth Structure Map Horizon A
2000
metre
3500
Fig. 9d
Fig. 9c
Orthrus-1
Fig. 7d
Fig. 7a
Fig. 7c
25 km
(b) RMS amplitude of Horizon A (+/- 17 ms)
Low
High
Straight lineations
Sinuous lineations, SU-1 contourite channel
Fig. 9d
Fig. 9c
Orthrus-1
Fig. 7d
Fig. 7a
Fig. 7c
25 km
(c)
W
E
B
A
100 ms
2.5 km
(d)
NW
SE
B
A
100 ms
2.5 km

862

863 Fig. 10

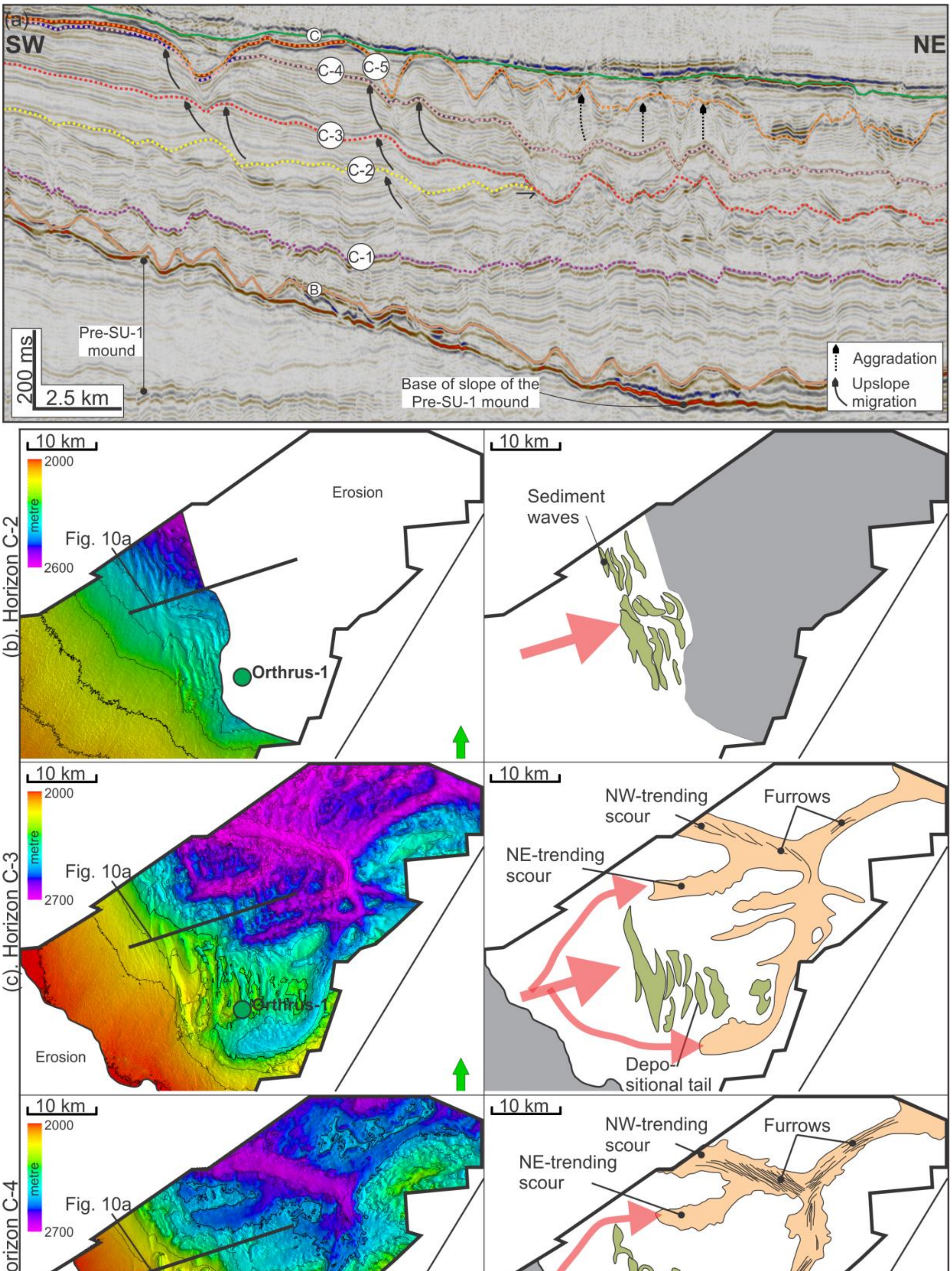

864

865 Fig. 11

866 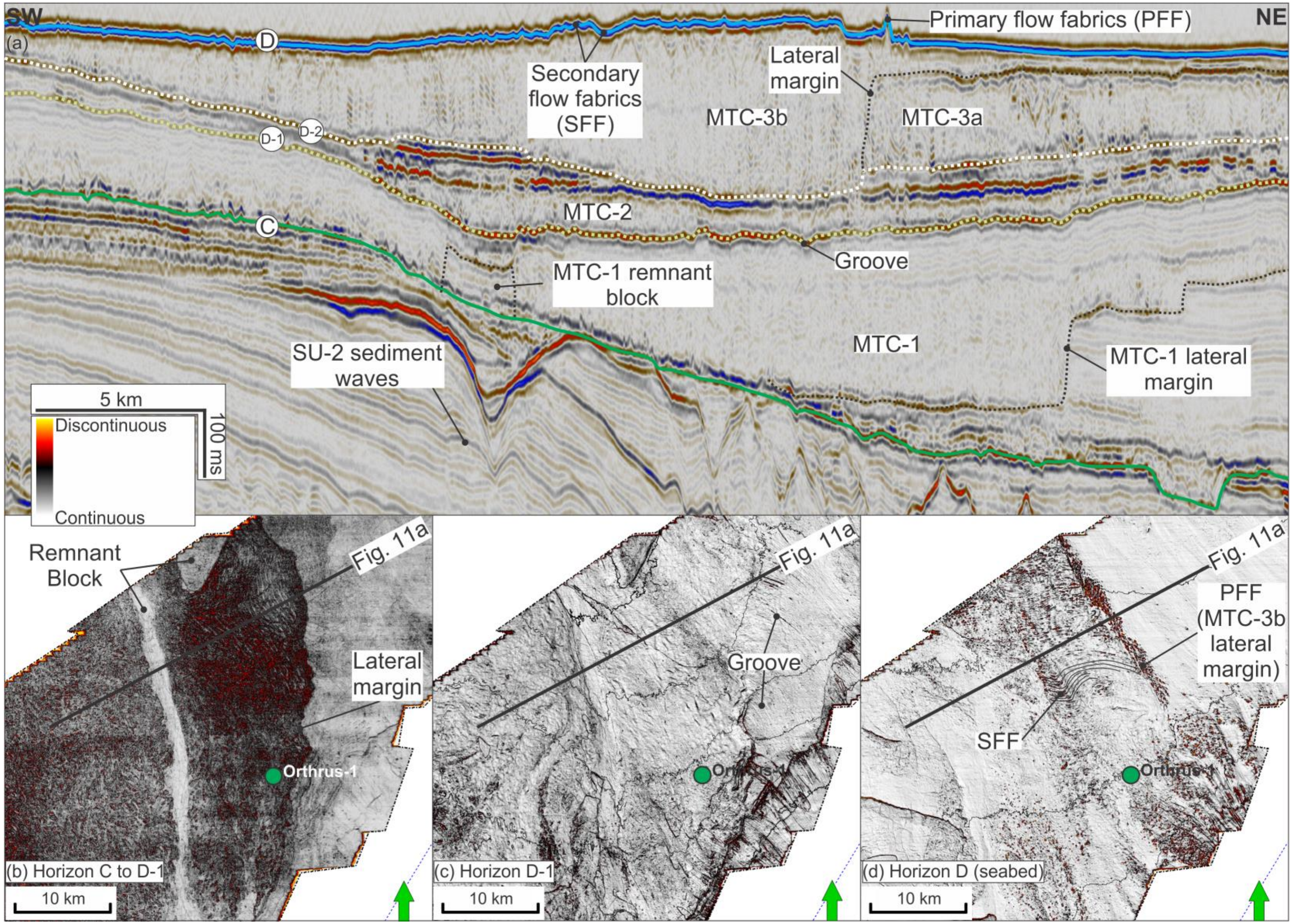

867 Fig. 12

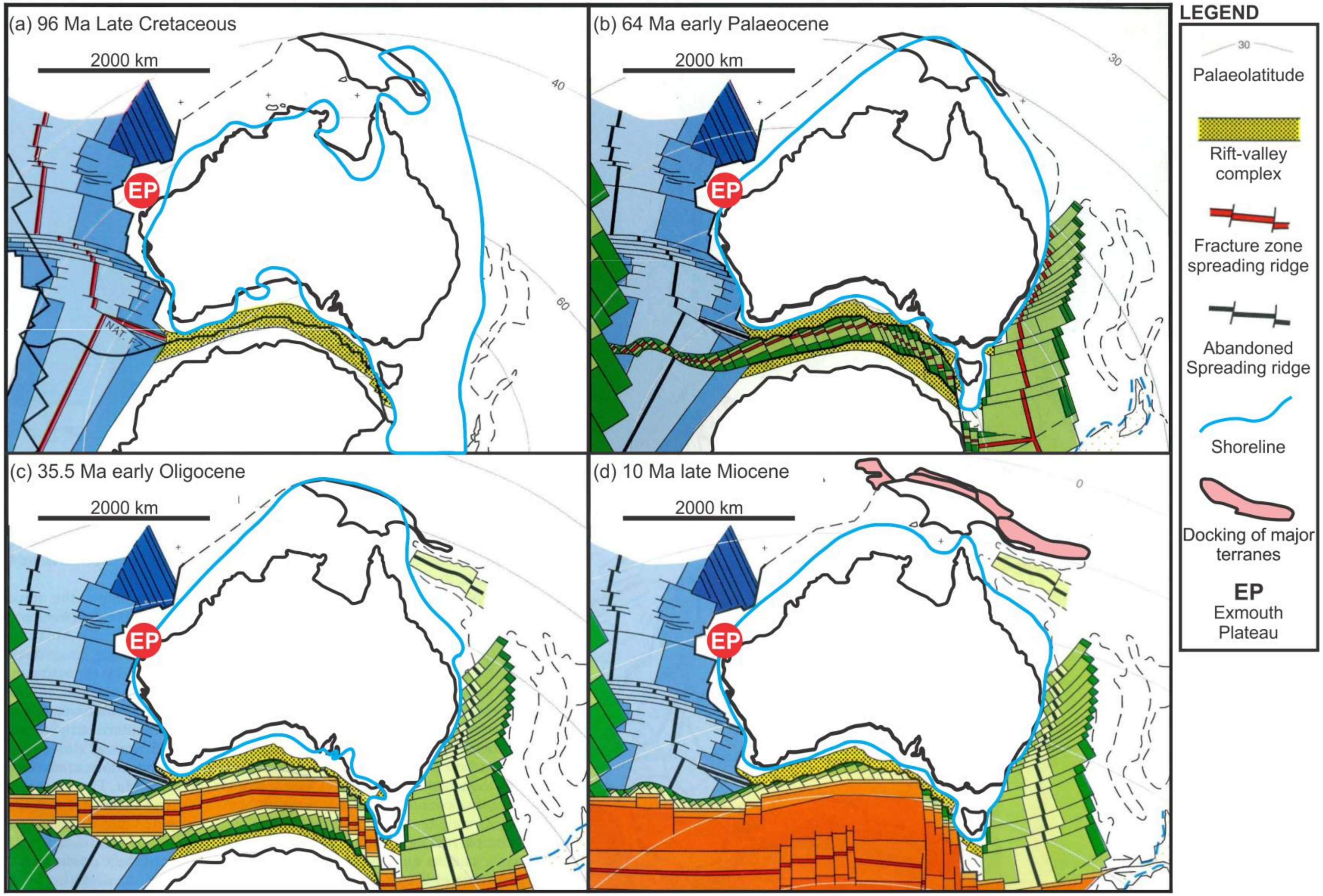

868